Capacity of Single-Hop Communication Links in Wireless Ad Hoc Networks

by

Filip S. Antic

Submitted to the Department of Electrical Engineering and Computer Science

in Partial Fulfillment of the Requirements for the Degree of

Master of Engineering in Electrical Engineering and Computer Science

at the Massachusetts Institute of Technology

August 2, 2004 [September 2004]

Author_____
Department of Electrical Engineering and Computer Science
August 2, 2004

Certified by_____
David H. Staelin
Thesis Supervisor

Accepted by_____
Arthur C. Smith
Chairman, Department Committee on Graduate Theses

Capacity of Single-Hop Communication Links
in Wireless Ad Hoc Networks
by

Filip S. Antic

Submitted to the
Department of Electrical Engineering and Computer Science

August 2, 2004

In Partial Fulfillment of the Requirements for the Degree of
Master of Engineering in Electrical Engineering and Computer Science

ABSTRACT

This thesis defines the capacity of single-hop communication links in wireless ad hoc networks as the transferable data rate over that link determined by the Shannon limit and by the fixed modulation scheme and bit error rate. The resulting capacity formulas are derived under the assumption of $r^{-3.8}$ path loss and uniform, but random, distribution of users. Rank of the link R is defined and included in the capacity formulas. After defining link capacity, the improvement of capacity is studied when different network components are implemented. These include successive interference cancellation (SIC), and multiple antenna arrays at the transmitting and the receiving end of the link. These strategies are then compared in terms of the dB improvement of capacity that they provide. Network parameter NP is defined in order to characterize spatial reuse in the network, and optimal network parameter is determined for maximizing link capacity in the process of dividing the network single frequency channel into equally sized subchannels.

Thesis Supervisor: David Staelin
Title: Professor of Electrical Engineering

Acknowledgements

I would like to express gratitude to professor David Staelin for giving me directions in my research and helping me shape this thesis. During my studies for Master of Engineering degree over the past year, he was a perfect advisor: helpful, resourceful, patient, and motivating. I enjoyed working under his supervision.

I would also like to express perpetual gratitude to my mother Danica and my future wife Zhenya for giving me endless support and understanding throughout my education. They made everything look easier and that is the reason why I dedicate this thesis to them.

I would also like to thank my fellow students Siddhartan Govindasamy and Keith Herring for working together on the project, discussing problems together, and helping each other in developing ideas. I took pleasure in working with them.

In addition to them, I would like to express appreciation to Daniel Bliss and Andrew McKellips from Lincoln Labs for weekly audio conferences where they gave many useful comments on my work, clarifying many research issues. I would also like to thank Dan for taking his time to occasionally visit us at MIT and have insightful conversations with us.

Table of Contents

Chapter 1:

Introduction and Background Information

1.1. Overview

This thesis is a part of a larger project underway in the Remote Sensing and Estimation Group (RSEG) of RLE at MIT. In this age of increasing use of radio spectrum for mobile communication, many research attempts (both theoretical and practical) were made to examine and find the best implementation of ad hoc wireless networks for wider use. Some of those attempts will be mentioned in later parts of this thesis. However, RSEG is concentrating on the problem posed by the increasing density of ad hoc wireless users in space, frequency and time, the foreseen future crowding problems. This group plans new systems for wireless ad hoc networks, including details about their infrastructure.

The systems they are analyzing include, among other things, protocols especially designed for this purpose. The current versions of system protocols include reservation signals for data channels, which are sent or not sent over side channels, beacon signals, and other versions. The system designs also include proposals for use of multiple antennas for blind signal separation and eliminating the signals that are discovered as interferers at the receiver's end of the data links Another purpose of multiple antennas will be to enhance the data rate communicated over the network links by directing the antenna gain in the direction of the user on the other end of the link, and decreasing the antenna gain in the directions from which the concurrent interfering signals come. This is the strategy of (partially) nulling the interfering signals and at the same time peaking up on the direction of the link, and is examined by simulations in this thesis.

This project is currently in its theoretical phase and, as a consequence, all results presented in this thesis are derived from simulations. The main purpose of this thesis was to find the theoretical limits to the data rate each user can get for himself in a crowded environment. I used two different approaches: the absolute theoretical limit defined by

the Shannon's binary channel capacity formula, and the data rate achievable when the modulation scheme and tolerable bit-error rate were fixed for all users in the network.

These theoretical limits and the information concerning how various components of the system influence these theoretical limits will help further theoretical and practical work on the larger project. Although the results depend on certain assumptions, for example the attenuation model and multi-antenna array constraints, the results can be easily modified as one assumes different things. For example, once the equipment now being developed by RSEG collects data concerning signal attenuation, a new different model can be discovered and incorporated in this work.

1.2. Related Work

Ad hoc wireless networks have been subject of many research efforts and some significant results have been achieved. The work of Gupta and Kumar [1] has shown that the transferable bit rate in multihop scenarios is $\lambda(n) = \Theta\left(\frac{W}{\sqrt{n \times \log n}}\right)$ for randomly chosen source and destination users, where n is the number of users of the network in a fixed area, W is the number of bits per second that each user alone can transfer, and the order Θ is defined by the equivalence relation $f(x) = \Theta(g(x)) \Leftrightarrow f(x) = O(g(x)) \wedge g(x) = O(f(x))$. Their result is valid for multihop communication, but it depends on the singlehop transferable data rate W. This thesis complements the result [1] of Gupta and Kumar in the sense that it determines W from various system components.

Multiuser detection is an important part of the design of future ad hoc wireless network systems, because it allows greater tolerance of receiver towards interference coming from other users in the network. Verdu did pioneering work in this field. In one of the first papers [2] he determined asymptotic bounds of multiuser detection method efficiency. Later, in [3], he and V. Poor described single-user detectors for multiuser channels, and determined optimal detectors under several different specific channel conditions such as power level of interferers and length of spreading codes of CDMA

signature waveforms. Lupas and Verdu went on in [4] to design a linear multiuser detector in a synchronous CDMA channel and prove that its performance is close to that of the optimum multiuser detector. This result was important since the computational complexity of the proposed linear detector was liner in the number of users, which made it applicable in real systems. Verdu and Lupas also proved in [4] and [5] that linear detectors are near-far resistant in synchronous and asynchronous CDMA channels and that result implied that linear detectors can be used in wireless communications since they could combat the large range of interfering signal power levels which is inherent in wireless systems. However, these papers did not consider blind multiuser detection, which does not require beforehand knowledge of signature waveforms. Honig, Madhow and Verdu considered this issue in [6] and proposed an adaptive linear multiuser detector which could do blind detection. In summary, this series of research efforts made huge progress in multiuser detection in wireless systems. The results of these mentioned papers are the foundation of successive interference cancellation, which is one of the methods whose contribution is evaluated in this thesis.

Other methods that can boost the data rate of a single link in an ad hoc network include usage of multiple antennas. Research done on space-time coding is summarized in [7] and [8]. Space-time coding is beyond the scope of this thesis, but can be examined in the future. There have also been efforts to determine the theoretical limits of Shannon capacity for multiple input multiple output (MIMO) systems, which are summarized in [9]. The loss of MIMO system capacity in the presence of environmental hindrances is examined in [10]. Papers [11] and [12] present some experimental results in this area for frequencies near the PCS frequency allocation (1790MHz).

Ad hoc wireless networks imply large interference between users, and multiple antennas can be used to detect and subtract interfering signals. [9] provides an overview of achievements in this area. In order to get good results, one must assume some knowledge of the MIMO channel, both from the transmitter and receiver's point of view. That includes the knowledge of either the exact state of the channel gain matrix, or the distribution of the matrix's coefficients, as well as the noise distribution. Those are big assumptions to make, but on the other hand this method is useful for detecting not only one signal among its interferers, but all of the signals received, one by one. The last

signal detected then has the strongest data rate (since the other signals are detected and subtracted beforehand). This method for our purpose is only important as a form of successive interference cancellation, looked at in this thesis. In contrast to this method, this thesis also contains examination of multiple antennas used for a different purpose – nulling the interferers. Instead of, or in addition to, detecting and subtracting the interfering signals, one can use the antenna inputs to boost the SINR of the receiver by choosing the best linear combination of inputs. More on this is presented in chapter 4.

In MIMO systems, the receiver needs to know the state of the channel gain matrix. The transmitter achieves that by sending the training signals for a period of time to the receiver before actually sending the data packet. The process is explained in [16] together with the recommended length of the training data package.

In addition to [1], there have been more papers on network capacity defined in the similar manner. Mostly their definition of network capacity was the aggregate data rate that could be transferred between randomly chosen users in the network under an arbitrarily defined protocol. In [13], a three-dimensional ad hoc network was examined, under a time division protocol and multihop routing. Although the bounds were correct in the limit, they were only correct up to a multiplicative constant. That is why this thesis is complimentary to the bounds determined for multihop routing if we want to estimate the achievable data rate at a more exact level.

One more thing that this thesis tries to do is determine how different components of network infrastructure influence achievable data rate (both on the link and on the network level). Extensive work on this subject has already been done in A. Goldsmith's group at Stanford. The paper [14] describes capacity regions of the network data rates when different network designs are used. It is notable that multihop data transfer brings large improvement over singlehop, and spatial reuse as well, while power control does not bring much improvement. The last method examined in [14] was successive interference cancellation (CIS), which in combination with multihop and spatial reuse achieves the greatest capacity region. This thesis, on the other hand, examines the use of multiple antennas for partial nulling of interferers (chapter 4) and makes further suggestions for spatial reuse in a large network (chapter 5).

Protocols for multihop routing are the next issue in finding the greatest data throughput in the network. [15] examines several protocols and ranks them according to their performance. The results found there say that: power control does not help much in data rate performance, CSMA/CA suffers from presence of weak links, a FIFO queuing rule is suboptimal, and two contention based protocols examined had the best performance. The two protocols were both time-framed, with control signals preceding the data packets.

1.3. Attenuation Model Assumptions

One of the crucial assumptions of this thesis is polynomial path loss with respect to transmitter-receiver distance. It is well known that in free space the intensity [Wm^{-2}] of electromagnetic waves is proportional to r^{-2}, where r is the distance from the transmitter. However, near land, buildings and other objects the situation is much more complicated. In such cases diffraction and reflection from various objects along the propagation path scrambles the field at the receiving point and the resulting field there is no longer the result of a single path line-of-sight electromagnetic wave. The resulting field very much depends on the position of all objects in the environment, buildings being the most influential factor. However, one can still talk about the average dependence of power on distance, and many experiments have confirmed that, on average, power is proportional to $r^{-\alpha}$ for some value of α. In [17] we find that α is usually between 2 and 4, and on average α=3.8. That is why in this thesis the simulations and results are presented for case of α=3.8 as that is the most referenced value for propagation constant:

$$P = A \cdot r^{-\alpha}, \text{ where } \alpha = 3.8. \qquad (1)$$

The justification for choosing polynomial path loss comes from several different experimentally developed path loss models. The first one is the Okumura-Hata model [18], where Hata has derived an equation based on numerous path loss curves that Okumura has measured in wide variety of conditions. Actually, there are several

equations, one for each of the following: large city, medium and small city, suburban area, and open area. All of them contain the dB path loss factor in the equation:

$$L_{PU}(dB) = \ \ldots \ + [44.9 - 6.55 \log_{10} h_b(m)] \log_{10} r(km) + \ \ldots , \qquad (2)$$

where r and h_b are distance from the base station and height of the base station. The result is polynomial path loss with respect to r, as claimed above. The only problem with this model is that it has been derived from measurements with h_b ranging from 30m to 100m, which are antenna heights larger than usual in ad hoc wireless networks. However, I have mentioned it here because it is the most accurate and complete experimental path loss model for urban environments in existence today.

Other researchers have also arrived at polynomial average path loss. In [19] we can find the results of a field experiment in the city of Helsinki, Finland. The researchers determined that at frequency 5.3 GHz path loss fits the polynomial model for both line-of-sight and non line-of-sight cases. For line-of-sight the attenuation coefficient oscillates from value *1.4* to value *3.5*, where value *1.4* is actually less than in the free space case, which is equal to 2. The reason for this is because a street can sometimes act as a waveguide and carry the power of electromagnetic waves over longer distances. On the other hand, for non-line-of-sight cases the attenuation coefficient oscillates between *2.8* and *5.9*, again around the value *3.8* used in this thesis. These experiments have been conducted with antennas of height 4m, 12m, and 2.5m, all of which being below rooftops, which makes the results more applicable to our purpose and ad hoc networks.

In addition to Okumura-Hata, there have been other empirical models. One of them is the COST-Walfisch-Ikegami model, which derives the path loss equation by taking into account the dominant role of multiple diffractions of waves over the rooftops of buildings [20]. This model also considers the width of the streets where the receiver is located and has a fine estimate of the roof-to-street segment of the signal path. However, what is important for us is the polynomial path loss that again appears in this model. For line-of-sight cases the path loss of the signal contains the factor:

$$L_p = \ldots + 26 \log_{10} r(km) + \ldots , \qquad (3)$$

which corresponds to the attenuation constant α=2.6. In the non-line-of-sight cases the path loss contains the factor:

$$Lp = ... + \begin{cases} 38 \log r(\text{km}), & \text{Htx} > \text{Hr} \\ \left(38 - 15\dfrac{\text{Htx} - \text{Hroof}}{\text{Hr} - \text{Hrx}}\right) \log r(\text{km}), & \text{Htx} < \text{Hroof} \end{cases}, \qquad (4)$$

where r, Htx, Hrx and Hroof are distance from receiver to transmitter, transmitter antenna height, receiver antenna height, and rooftop height, respectively. The corresponding value of attenuation constant here is α=3.8 minus a correction factor for the case when transmitter is below the rooftops. From here we conclude that this model supports the assumption of polynomial path loss and the choice of attenuation constants for the simulations and experiments.

Even though on-average path loss can be considered polynomial, there is evidence to believe that this assumption is overly simplified. If we look at the research results in the area of designing microcellular telecommunications systems in big cities, we find that the power attenuation greatly depends on the street pattern. In the paper [21] the boundary of regions with fixed path loss assumed a diamond shape in the rectangular parts of the streets of Boston, as opposed to circular pattern one would expect from polynomial path loss with respect to distance. The corners of the diamond shaped figure extended in the direction of the streets on which the transmitter was located, which means that the attenuation was stronger across the building blocks and weaker along the streets. This effect was evident for the frequencies on which the research concentrated, 2GHz and 6GHz, which also happen to be very close to the candidate frequencies for allocation to ad hoc wireless networks studied in this thesis (2GHz and 5GHz). The same paper also examines pattern of attenuation in the downtown Boston area, which has curvilinear instead of rectangular street pattern. In this case the boundary figure assumes an irregular circular shape, supporting evidence for the polynomial path loss model.

There is another example why polynomial path loss could be considered excessively simplified. In [19], experiments were conducted at 5.3GHz, again very close to the candidate frequency for application of ad hoc networks. One of their observations was the dramatic change in path loss when the receiver turned around the corner from the street where the transmitter was located to the street perpendicular to it. The path loss pattern was polynomial in the first street and also in the second street, but between them there was a sharp cutoff of 26dB.

This effect again proves that the street pattern greatly influences the path loss. However, the simplification of putting complicated multiple diffractions and refractions along streets and buildings into just one constant α, was enough to decide to neglect these objections for the time being. The next research step could be incorporating street geometry into the simulations and path loss model. One approach could be to include another constant or random variable to supplement α in description of propagation loss, and another one could be to distort the Euclidian space where the users and interferers are located in order to accommodate street shape dependence. In such research attempt users that are located along the same street could be considered closer than their actual distance, and the users isolated from each other with many obstacles could be considered farther than their actual distance; just so they all fit into the $r^{-\alpha}$ attenuation model used in this thesis.

Chapter 2:

Metric Definition

2.1. Significance of Metric

We would like to be able to compare two given infrastructures of an ad hoc wireless network. The ad hoc network is always given to us, because we cannot change the geographical distribution of users or the physical characteristics of the environment. However, what we can do is design the infrastructure of the ad hoc network so that the owner of the network is maximally satisfied. The infrastructure includes but is not limited to the antenna characteristics, blind signal separation methods, and the protocol that the users have agreed to use while transmitting data over a link. All these characteristics can be changed to improve the satisfaction of the users in the network, but they also have their cost of implementation. That is why we need a tool to predict how much exactly each change in every infrastructure design detail contributes to the total performance of the network. We need a scale on which we could rank the overall performance of different infrastructures for the same ad hoc network.

2.2. Requirements

The most natural metric to use for communication systems is the data rate of the users, since data transfer is the basic purpose of such systems. In this thesis I examine the data rate that can be transferred over one link, from the transmitter to the receiver, with no consideration of multihop strategy. The basic model of transfer that I consider is one transmitter, one receiver, and other users, whose transmissions interfere at the receiver with the desired signal coming from the transmitter. The interference can then either be eliminated by successive interference cancellation, or simply added to the thermal noise and considered as additional noise.

There are two different ways that we can use to determine transferable data rate over a link. One is to use Shannon's binary channel capacity, which would give us the maximum data rate over the link. However, even though this limit is a useful value to know, it is not practically achievable in wireless systems, since that would require infinite delays while recovering data. That is why I considered another way of determining data rate over a link. The other approach would be to assume a fixed modulation scheme and fixed bit-error rate that can be tolerated, and calculate the data rate from there. This second approach is closer to practical implementation than taking the Shannon's limit, but, nonetheless, both approaches for calculating data rate are considered in this thesis, the first one as the absolute limit, and the second one as practically achievable data rate.

A higher data rate makes the system more appreciated, but we must consider the tradeoffs as well. A higher data rate is likely to increase the cost of system implementation, and the cost is distributed over different components of the system. That is why we would like to have a way of determining how much each component of the system influences the data rate in an average link in the network. When one has such information one can decide which component of the system is best to invest in, in order to get maximum improvement of the data rate at minimum total cost.

In the later part of this chapter, I present the equation that calculates the data rate over a link as a function of different system components characteristics. That equation exactly serves the goal of making transparent which parts of the system are best to invest in for achieving optimum data rates on communication links in the network. In chapters 3 and 4 I describe how much successive interference cancellation strategy and multiple antennas, which are some of the components of the system to consider, change the data rate of links in the network through the equation defined in this chapter.

Before I derive the equation, let me emphasize some important assumptions about the ad hoc wireless networks that we consider. The first one is that a network consists of users distributed uniformly in a plane, but randomly, some of them being receivers and others transmitters. A user can only be a receiver or a transmitter at a certain point of time, and both of them are distributed in the plane with the same area density. Data transfer in such a network happens over single hop links between receivers and transmitters. All transmitters transmit in the same frequency band, and their signals are

considered as interference at all receivers except for the one receiver that is expecting the signal. All signals attenuate according to the polynomial attenuation model described in the previous chapter, with attenuation constant α. These assumptions explain most features of the network, but in order to get a sense of what is the data rate on a link, we need to know the link length relative to the distances to the interferers in the area.

2.3. Rank and Network Parameter

Rank of the link is a measure of relative distance from the transmitter to the receiver, relative to the distances from the receiver to the other transmitters in the area. The exact definition is as follows:

In a link of rank R the receiver is listening to the R^{th} closest transmitter, while all other transmitters are considered to be interferers to that receiver.

Since all transmitters are assumed here to have equal power, the R^{th} closest transmitter is also the R^{th} strongest if all antennas are isotropic.

Rank in combination with knowledge of area density of transmitters (ρ) is all the information that we need about the geographical distribution of transmitters (both desired and interfering) around the receiver, for $R \geq 2$. For $R = 1$ you might use the network parameter, which is defined a few paragraphs below. One can also determine roughly what is the link length (r) from the knowledge of rank and area density of transmitters in the area (for $R \geq 2$):

$$R \cong \rho \cdot \pi \cdot r^2$$

$$r^2 \cong \frac{R}{\rho \cdot \pi}$$

$$r \cong \sqrt{\frac{R}{\rho \cdot \pi}}, \qquad (5)$$

where ρ is equal to $\#transmitters/m^2$ in the network.

From this connection between r and R, and the fact that power of the received signal has a polynomial dependence on r, we can derive a further connection between R and the signal power level at the receiver. This fact is going to be used in the derivation of the equation for data rate over a link of rank R later in this chapter. For $R=1$ formula (5) cannot be used for determining the power level of the signal at the receiver, and in that case other methods, such as using the network parameter, need to be used for calculating the data rate over the link. Other information that we need in order to find the data rate over the link include the interference level at the receiver, which is equal to the sum of all individual signal powers coming from interfering transmitters surrounding the receiver. For calculating individual interfering signal powers we can still use formula (5) in combination with the polynomial attenuation model, but only for rank of interferer $R \geq 2$. The largest interferer, with rank $R=1$, does not obey equation (5) and other methods need to be used in order to estimate its power level.

Rank was defined above for a single link, but we can also talk about rank of a network, or part of a network. Here is the definition:

In a network, or part of a network, of rank R, all links have rank R.

This is a loose definition, since strict application in practice would mean that sometimes two or more receivers listen to the same transmitter at the same time, because the R^{th} closest transmitter from one receiver can at the same time be the R^{th} closest from another receiver. Networks of different rank are visually distinguishable, as shown on the images below. All links in these images have the same rank, so the overlapping can be noticed, which should not happen in practice. However, the idea here is to get a sense of how long are the links in the network relative to the distances between users in a network with uniformly, but randomly, distributed transmitters and receivers.

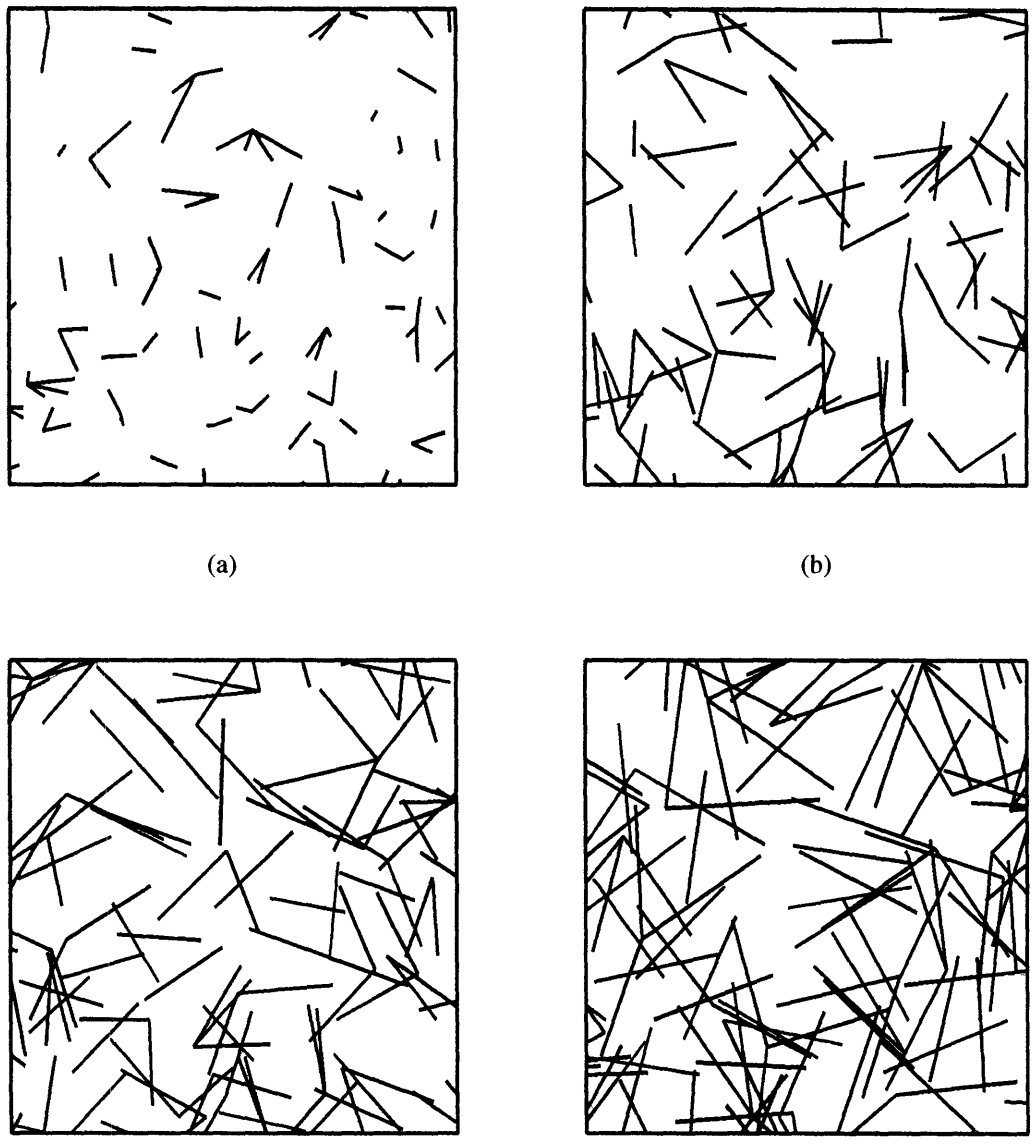

(a) (b)

(c) (d)

Figure 1: (a) Network of rank $R = 1$; (b) Network of rank $R = 5$; (c) Network of rank $R = 10$; (d) Network of rank $R = 20$.

In addition to rank, I consider another index value that characterizes link length relative to distances to interferers in the neighborhood. It is called the network parameter (*NP*) and the definition is as follows:

$$\boxed{NP \equiv r \cdot \sqrt{\rho}}, \tag{6}$$

where r is the link length and ρ is the area density of transmitters around the receiver. This definition is useful for rank $R = 1$ networks, because that is the only time the duality relation (7) does not hold. One can easily derive the duality relation (7) from equations (5) and (6).

$$NP \cong \sqrt{\frac{R}{\pi}}, \text{ for } R \geq 2. \tag{7}$$

Some example values for *NP* are given in Table 1, with reference to rank values that are associated with them. Since the notion of rank is intuitively clearer than the notion of network parameter, I will use rank in all cases where I can, to describe the distance of the transmitter from the receiver in a link, or a set of links. That will be the case in chapters 3 and 4, while in chapter 5 I use the network parameter to describe the optimum division of one frequency channel into many.

Table 1: Correspondence between values of rank *R* and network parameter *NP* for $R \geq 2$.

R	*NP*
2	0.798
5	1.262
10	1.784
20	2.523

2.4. Formula Derivation

Capacity

In the beginning of the chapter I mentioned two ways of calculating the bit rate that can be transferred over a link in the network. One approach is to evaluate Shannon's capacity limit, and the other approach assumes a certain bit error rate and a modulation

scheme, from where we can derive the bit rate over the link. Resulting bit rates from both approaches are useful to know, but the first one is the absolute limit in the bit rate, while the second one would be more applicable to the actual systems.

The first approach, taking Shannon's bit rate, is simple; one just applies the Shannon's capacity formula, bearing in mind how noise and interference, as well as the signal power level at the receiver's end of the link, can be calculated from the parameters of the system:

$$C = \log_2(1 + SINR) \left[\frac{\#bits}{\sec \cdot Hz}\right], \tag{8}$$

where C is the limit on how many *bits* can be transferred over the link per *second* and per *Hz* of bandwidth; and *SINR* is the ratio of signal power level and the sum of noise power and total interference power in the same bandwidth.

In the other approach, one does not take the absolute Shannon limit, but instead the limit under the assumption of a fixed bit error rate and a certain modulation scheme. For example, in this thesis I have decided to concentrate on bit error rates at around 10^{-2}, which under the BPSK modulation scheme requires $\frac{E_b}{N_0}$ at the level of approximately $5dB$ [22]. From here we can derive the dependence of achievable bit transfer rate in the system on the SINR at the receiver's end of the link. The equation (9) at the end of this derivation presents the achievable bit rate normalized by time and bandwidth. The starting equation is:

$$\frac{E_b}{N_0} = \frac{\frac{E_{signal}}{\#bits}}{\frac{E_{N+I}}{\Delta t \cdot B}},$$

where E_b is energy per bit, N_0 is power spectral density of *noise+interference*, E_{signal} is the total energy that the receiver gets during the time *#bits* are transferred to the receiver, and E_{N+I} is the energy the receiver gets from thermal noise and interference during time Δt and over bandwidth B. The next step takes us to the bit rate capacity:

$$\frac{E_b}{N_0} = \frac{\frac{E_{signal}}{\Delta t} \cdot \frac{1}{\frac{\#bits}{\Delta t}}}{\frac{E_{N+I}}{\Delta t} \cdot \frac{1}{B}}$$

$$\frac{E_b}{N_0} = \frac{W_{signal}}{W_{N+I}} \cdot \frac{1}{\frac{\#bits}{\Delta t \cdot B}}$$

$$\Rightarrow \frac{E_b}{N_0} = SINR \cdot \frac{1}{C}, \text{ where } SINR = \frac{W_{signal}}{W_{N+I}} \text{ and } C = \frac{\#bits}{\Delta t \cdot B}.$$

In the last two lines W_{signal} and W_{N+I} are power levels of the signal and the sum of noise and interference at the receiver, respectively. The conclusion of this derivation is:

$$C = SINR \cdot \frac{1}{E_b / N_0} \left[\frac{\#bits}{\sec \cdot Hz}\right], \qquad (9)$$

where *SINR* is the signal-to-interference+noise ratio at the receiver's end of the link. As mentioned above, the value for $\frac{E_b}{N_0}$ that is reasonable to assume is 5dB.

SINR

Formulas (8) and (9) both contain *SINR* as the key parameter, and that parameter needs to be estimated in order to get useful data rate equations from (8) and (9). There are certain assumptions that I use when estimating *SINR*. The first one is uniform distribution of transmitters in the area around each receiver. They are distributed randomly with area density $\rho \left[\#users/m^2\right]$, and the receiver is listening to only one of them, with rank *R*, while the others are considered to be interferers to the receiver. All transmitters are considered to transmit the same power with their antennas (P_{tr}) and the power attenuation model is polynomial, as described in chapter 1:

$$P_{rec} = A \cdot r^{-\alpha} = P_{tr} \cdot \left(\frac{r}{r_0}\right)^{-\alpha} \tag{10}$$

where P_{rec} and P_{tr} are received and transmitter power, A and α are constants in the attenuation model, and r_0 is a constant that connects P_{tr} and A. In addition to these assumptions, I assume that all users in the network have isotropic dipole antennas, which have equal antenna gain in all directions in the plane. For now I consider that each user has only a single antenna, and in later chapters we can see what happens when one provides each user with multiple isotropic dipole antennas.

An important assumption in addition to these is neglecting the thermal noise at the receiver. The reason for this decision is simplification of the expression for *SINR* because when you do not have thermal noise in the equation, the parameters P_{tr} , A, and r_0 from (9) appear in both the numerator and the denominator of the expression for *SINR* and they cancel out. Justification for this decision lies in the fact that one can always increase the power level of all transmitters in the network until the thermal noise is negligible in comparison to the level of interference.

The assumptions made in the previous two paragraphs make it possible to estimate *SINR* as a function of numerical parameters describing the network. The expression for the *SINR* (we could also call it *SIR*, since the thermal noise is neglected) is now:

$$SINR = \frac{W_{signal}}{W_{interf}} = \frac{A \cdot r^{-\alpha}}{W_{interf}}, \tag{11}$$

where W_{signal} and W_{interf} are signal power level and interference power level, respectively. The first equality in (11) is completely true only when thermal noise is zero, but we consider this equation to be an accurate enough approximation. In calculating the expression for W_{interf} I have tried two approaches, described below. Only the second approach gave a satisfying result, and that is why I use it for the derivation of the final formula for *SINR*.

Integration

The first approach was to integrate the power that the receiver gets from "blurred" interferers in the network. In other words, I considered concentric rings centered at the receiver, rings of width dr, radius r and area $2\pi \cdot r \cdot dr$, and assumed that in one such ring there were $dN = \rho \cdot 2\pi \cdot r \cdot dr$ users, which was an infinitesimal value, and did not have to be an integer. Using infinitesimal values for power $dW_{interf} = A \cdot r^{-\alpha} dN$, I could integrate over area in the ring from the radius r_1 to the radius r_2 in order to get total interference power that comes from interferers between radius r_1 and radius r_2:

$$\begin{aligned}
\Delta W_{interf}(r_1, r_2) &= \int_{r_1}^{r_2} dW_{interf} \\
&= \int_{r_1}^{r_2} A \cdot r^{-\alpha}\, dN \\
&= \int_{r_1}^{r_2} A \cdot r^{-\alpha} \cdot \rho \cdot 2\pi \cdot r\, dr \\
&= \begin{cases} A \cdot \rho \cdot 2\pi \cdot \dfrac{1}{-\alpha+2} r^{-\alpha+2}\Big|_{r_1}^{r_2}, & \text{for } \alpha > 2 \\ A \cdot \rho \cdot 2\pi \cdot \ln r\Big|_{r_1}^{r_2}, & \text{for } \alpha = 2 \end{cases}
\end{aligned} \tag{12}$$

Total interference power level could be estimated from (12) when one substitutes 0 and $+\infty$ for r_1 and r_2:

$$W_{interf} = \Delta W_{interf}(0, \infty). \tag{13}$$

However, it turns out that when you combine (12) and (13), the resulting interference power is infinite, $W_{interf} = \infty$, for both $\alpha = 2$ and $\alpha > 2$.

One could avoid infinite interference if only $\alpha > 2$ is used and there are no interferers in the neighborhood of the receiver within radius r_1 :

$$W_{interf} = \Delta W_{interf}(r_1, \infty). \tag{14}$$

In this case the result for total interference W_{interf} heavily depends on the radius r_1 :

$$W_{interf}(r_1) = A \cdot \rho \cdot 2\pi \frac{1}{\alpha - 2} \frac{1}{r_1^{\alpha-2}}. \tag{15}$$

The result (15) is better than infinity, but it is not good enough, because the value of r_1 is then excessively important for determining the total interference.

In conclusion, integrating infinitesimal interference over the plane did not give good results. Either the calculated interference was infinite, or it heavily depended on the size of the "forbidden" neighborhood around the receiver. That is why I did not continue to use this approach in order to get the estimate for W_{interf} and *SINR*.

Monte-Carlo Experiments

The second approach for calculating W_{interf} and *SINR* was to use Monte-Carlo trials. The actual formula for *SINR* that I used was:

$$SINR \equiv \frac{A \cdot r^{-\alpha}}{\sum_i A \cdot r_i^{-\alpha}}, \tag{16}$$

where r_i were all interferers in the network. In each experiment I used 1000 transmitters randomly distributed in the network around the receiver, with area density $\rho \left[\#users/m^2\right]$; one of them was the desired transmitter and all others were interferers. I used only $\alpha = 3.8$ since $\alpha = 2$ would in theory lead to infinite interference, which can be concluded from infinite upper integration limit in the second part of (12). For $\alpha = 3.8$ the peripheral interferers do not contribute much to the total interference, so I distributed the transmitters in a square around the receiver and did not care about the edge effects. The total interference coming from outside of the square was estimated by using (14) and (15), and the resulting interference level was less than 0.1%, a negligible amount.

One can see from (16) that the *SINR* does not depend on the power level of the transmitters, since A cancels out from the equation, and also does not depend on the

density of the users. The proof of the second claim is the fact that the scale of r and r_i also cancel out. In the further derivation of the *SINR* expression, I first cancel A from numerator and denominator in (16), and then use (5) in order to eliminate the dependence on r:

$$SINR \cong \frac{r^{-\alpha}}{\sum_i r_i^{-\alpha}}$$

$$SINR \cong \frac{\left(\sqrt{\frac{R}{\rho \cdot \pi}}\right)^{-\alpha}}{\sum_i r_i^{-\alpha}}$$

$$SINR \cong R^{-\alpha/2} \cdot \frac{\left(\frac{1}{\rho \cdot \pi}\right)^{-\alpha/2}}{\sum_i r_i^{-\alpha}}. \qquad (17)$$

The expression (17) for *SINR* of the link contains two parts. The first one, $R^{-\alpha/2}$, captures the necessary information about the relative link length, following the definition of rank of the link at the beginning of this chapter. The second part of (17) is a number that depends primarily on the attenuation constant α and slightly on the link rank R, while it does not depend at all on the area density of the users ρ (see (18)). The fact that the second part of (17) does not depend on ρ is very useful because it makes *SINR* a function of only R and α, two very basic parameters.

In order to calculate the second part of (17) I used Monte-Carlo experiments. Here is the description of the experiment: in one trial I distributed 1000 interferers in a square area around the receiver, with the density $\rho \left[\#users/m^2\right]$. I used different densities and the result did not depend on the choice. The attenuation constant was $\alpha = 3.8$, and for such an attenuation model the edge effects were negligible, so the summation $\sum_i r_i^{-\alpha}$, which in theory should include all interferers in an infinite plane, was well approximated by the 1000 users in a square around the receiver (the estimated error by using (14) was less than 0.1%). The resulting formula for the *SINR* on the link was:

$$\boxed{SINR \cong R^{-\alpha/2} \cdot \delta(R) \cdot \gamma}, \qquad (18)$$

where γ was a constant whose value was calculated to be $\boxed{\gamma = 0.5473}$, and $\delta(R)$ was a correction factor whose values are given in Table 2.

The constant γ here is exactly equal to the estimated second part of the right-hand side of (17), the quantity we were looking for, but only in the case when all transmitters from the network were considered to be interferers and were included in the summation $\sum_i r_i^{-\alpha}$. However, the definition of rank in this thesis says that for a link of rank R the R^{th} closest transmitter is considered to be the transmitter that the receiver is listening to, and, thus, it should be excluded from the total interference level. In other words, we need to exclude the transmitter from the summation $\sum_i r_i^{-\alpha}$, which corresponds to adding a correction factor $\delta(R)$ in the formula (18). The values for the correction factor do not change the result very much, at most by 19% when $R = 2$, and the effect practically loses significance very quickly as R grows. In the Table 2 the results from the experiment show how the correction factor changes with R, and one can see how it is a decreasing function of R and how its values approach 1 as R increases.

Table 2: The correction factor $\delta(R)$ as a function of R.

R	2	3	4	5	6	7	8	9	10	11
$\delta(R)$	1.19	1.10	1.06	1.04	1.03	1.02	1.02	1.02	1.01	1.01

Formula

The expression (18) for *SINR* is simple and depends only on rank R of the link, and implicitly on the assumption $\alpha = 3.8$. It is valid for the case of randomly distributed transmitters in the network with any density, with all transmitters having the same power level and negligible thermal noise at the receiver's end. Both transmitters and receivers are assumed to have isotropic dipole antennas that have the same gain in all directions in

the plane. Under all these assumptions, we have the expression for *SINR* and we can plug in that result into the two formulas for link capacity (8) and (9).

The capacity that was derived from the Shannon's limit is now

$$\boxed{C = \log_2\left(1+\delta(R)\cdot\gamma\cdot\beta\cdot R^{-\alpha/2}\right) \quad \left[\frac{\#bits}{\sec\cdot Hz}\right]}, \tag{19}$$

and the capacity that was derived after assuming error rate at 10^{-2} and BPSK modulation scheme is

$$\boxed{C = \delta(R)\cdot\gamma\cdot\beta\cdot R^{-\alpha/2}\cdot\frac{1}{E_b/N_0} \quad \left[\frac{\#bits}{\sec\cdot Hz}\right]}, \tag{20}$$

where R is the rank of the link (under the condition $R \geq 2$); also $\gamma = 0.5473$, $\delta(R)$ is given in Table 2, $\frac{E_b}{N_0} = 5dB = 10^{5/10}$, and β is the parameter that captures the effect of successive interference cancellation and multiantenna nulling described in chapters 3 and 4. The value of β for the time being is 1, but in the following chapters its value will be greater than 1, thus improving the link capacity.

While we consider $\beta = 1$, we can use (19) and (20) to find the link data rate per Hz and plot it as a function of R. The resulting plots are shown in Figures 2, 3 and 4.

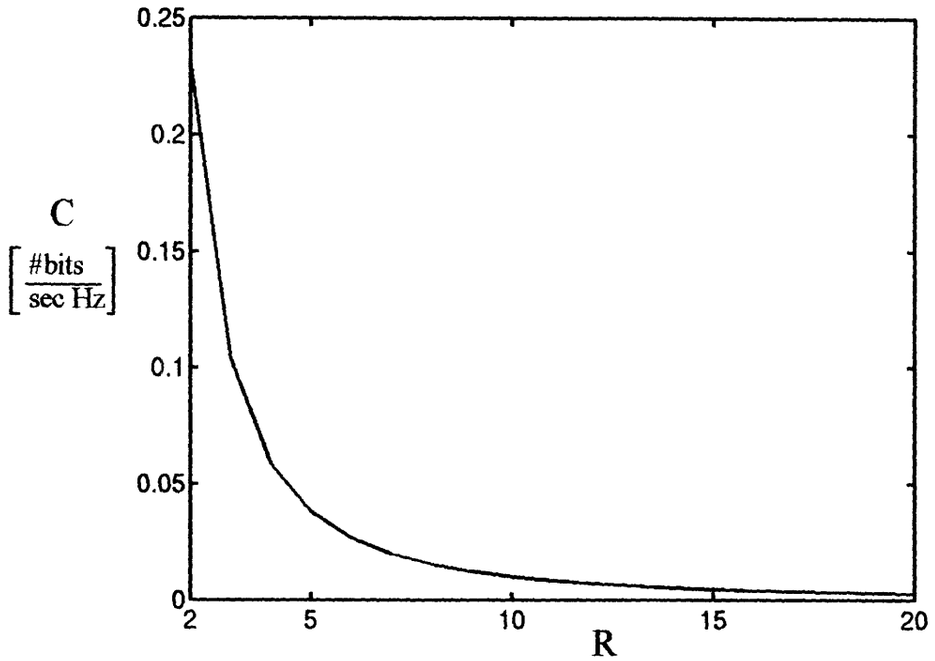

Figure 2: Capacity of a link in the network vs. rank of the link. This capacity corresponds to the Shannon's capacity limit (data rate per Hz), calculated by formula (19).

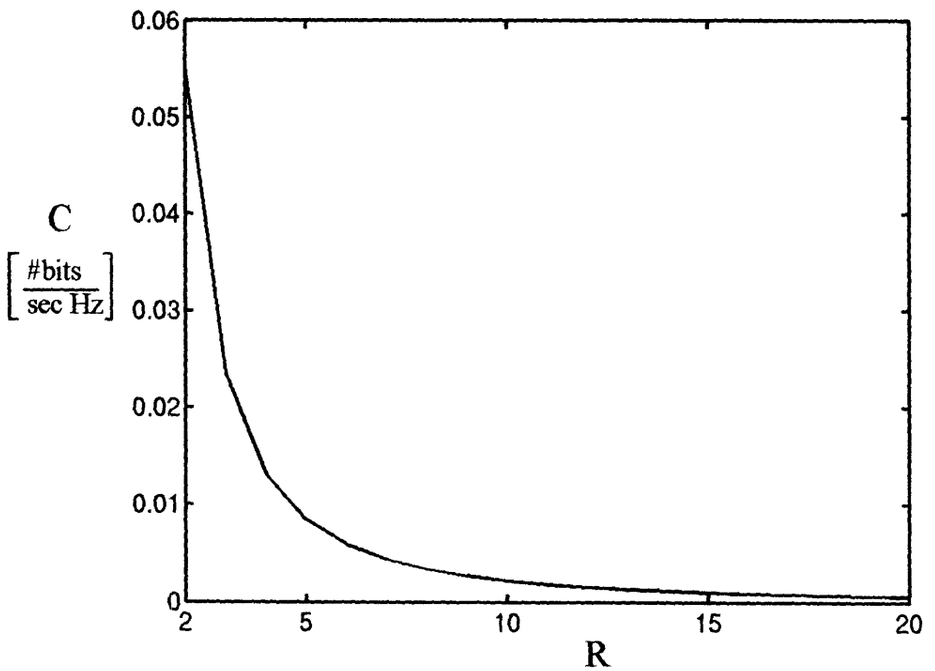

Figure 3: Capacity of a link in the network vs. rank of the link. This capacity corresponds to the data rate per Hz, available under BPSK modulation scheme and with tolerable bit error rate 10^{-2}. The capacity is calculated by formula (20).

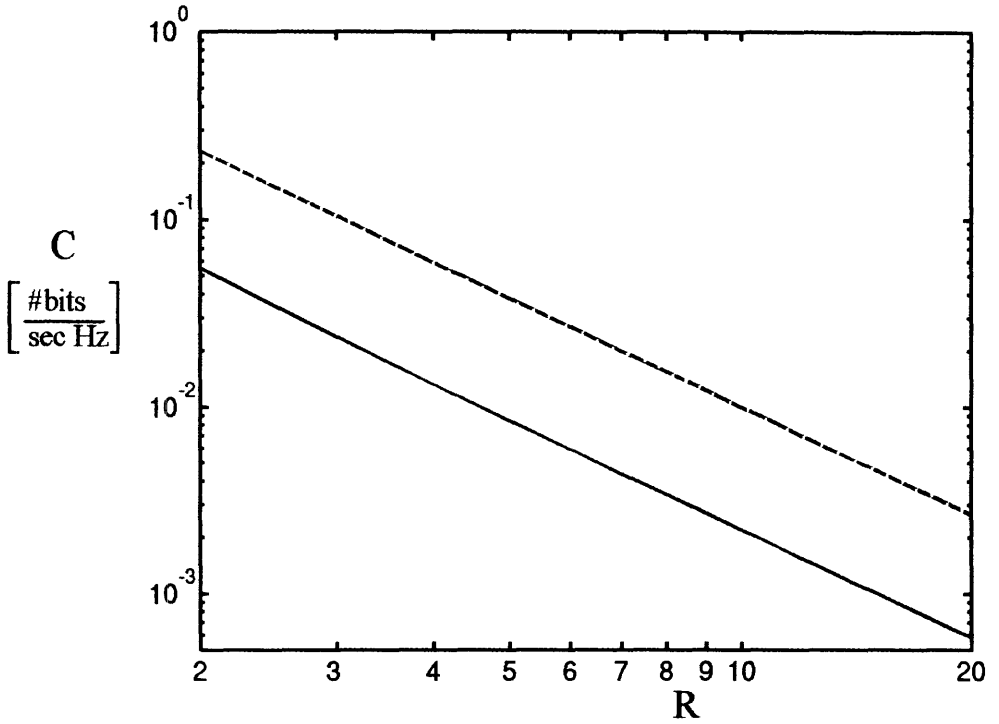

Figure 4: Capacity of link vs. rank of the link, on a log-log scale. The top (dashed) curve corresponds to the capacity in Figure 2, while the bottom (solid) curve corresponds to the capacity in Figure 3. The difference between the curves is *6.2dB* for *R=2*, and *6.4dB* for *R=20*.

In conclusion, this chapter introduces the notion of rank of the link R and rank of the network, definition of the network parameter *NP*, and the connection between R and *NP*. I used those definitions and under certain assumptions derived two types of link capacity (given by formulas (19) and (20)) that depended only on the value of R and implicitly on the attenuation constant α. The assumptions I made were: uniform distribution of transmitters in the area, negligible thermal noise, polynomial path loss with attenuation constant $\alpha = 3.8$, all users in the same bandwidth, and single isotropic dipole antennas at each user. Under those conditions, formulas (19) and (20) can be used with $\beta = 1$, and once we introduce successive interference cancellation in chapter 3 and multiple antennas in chapter 4, the value for β can increase and we can see how much improvement each of these strategies bring to the link capacity, which is considered to be the base metric for measuring the performance of the system.

Chapter 3:

Successive Interference Cancellation

The isotropic dipole antenna case considered in the previous chapter was the base for deriving the two forms of capacity formula, (19) and (20), but the capacity that is determined this way is by no means the maximum achievable capacity. The factor β in formulas (19) and (20) captures the effects of using successive interference cancellation (SIC) and multiple antennas. While multiple antennas will be discussed in chapter 4, in this chapter I concentrate on SIC.

I do not go into the technical detail how the SIC is conducted, and do not determine what are its limits, but instead, I determine what are its effects on the capacity over a link in the wireless network. I assume that the description of the network is the same as in previous chapters, and that formulas (19) and (20) correctly calculate link capacity in the network. When no SIC is used, the factor β is equal to 1, and all interferers in the network are included in the total interference level.

The SIC strategy that I assume here means that the receiver detects the interfering signals from the n strongest interferers, and subtracts them from the total interference level. As a consequence, *SINR* increases, which is then followed by the increase of the link capacity. The effect of *SINR* increase is captured in the multiplier β, which is equal to the ratio of the *SINR* after and before SIC. I plotted in Figure 5 the dB value of β (improvement over its original value 1) vs. the number of subtracted interfering signals.

The source of these results were Monte-Carlo trials designed to measure the total interference, as well as interference after subtracting up to 20 strongest interferers from the total sum. Again, for each trial I used 1000 interferers distributed randomly in a square field surrounding the receiver. The attenuation model was polynomial with $\alpha = 3.8$, which made the edge effects negligible. I considered the thermal noise much lower than the interference level, so I did not include it in the expression for *SINR*. There were 1000 trials for every number of cancelled interferers, and from them I determined the average value for β as well as the standard deviation, which is plotted in Figure 5. I

also determined the average and standard deviation for the capacity values, which are plotted in Figures 5-11.

The practical definition of capacity (with fixed bit error rate and $\frac{E_b}{N_0} = 5dB$) is proportional to *SINR* and β (see (20)), and as a consequence, the dB improvement of this capacity is the same as the dB improvement of β. The results for both β and capacity defined in (20) is given in Figure 5.

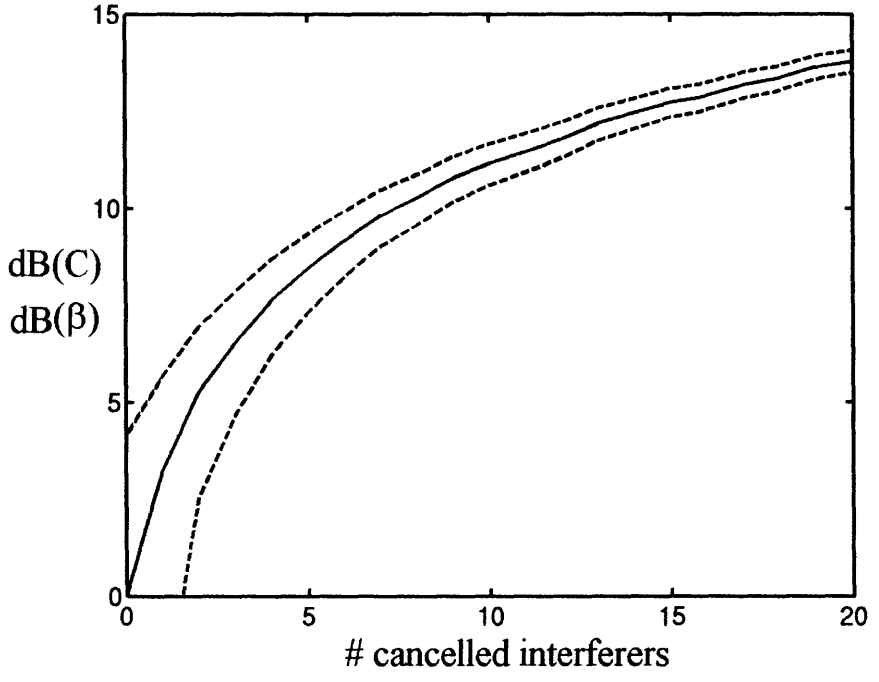

Figure 5: Improvement in dB of β and link capacity as defined in (20), plotted against the number of interferers subtracted in the SIC strategy. The solid line is the average result, and the dashed lines correspond to the average plus or minus the standard deviation of results.

The other definition of capacity, which was derived from the Shannon' s limit and described in (19), is proportional to the logarithm of an expression containing β. That is why the dB improvement of such capacity depends on the original capacity value. In our case, since the capacity in (19) depends on the rank R of the link, it means that the dB improvement of capacity also depends on the rank of the link. That is why the results are presented for various values of R. These results are shown in the Figures 6-10.

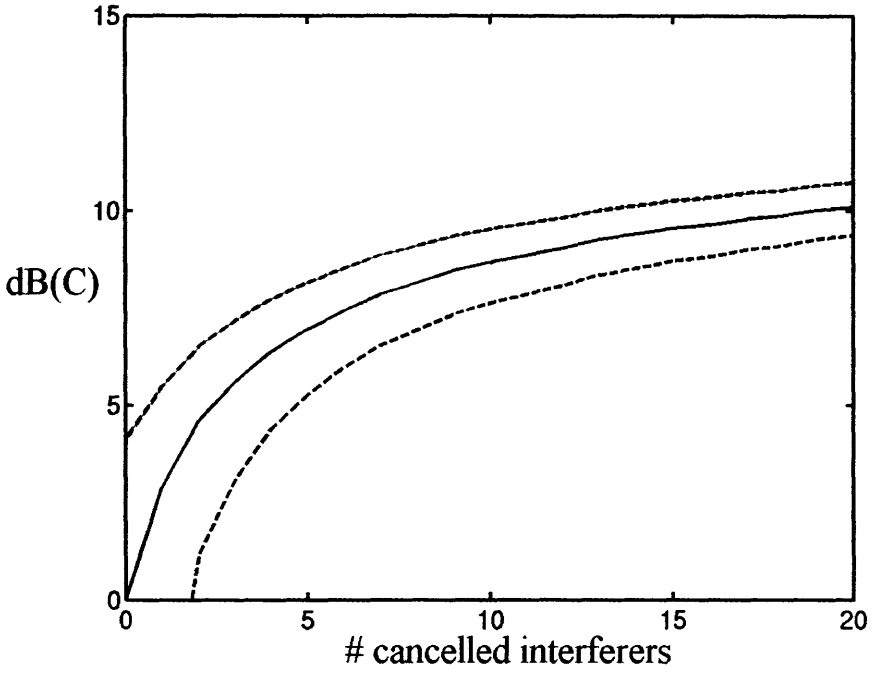

Figure 6: Improvement in dB of link capacity as defined in (19), plotted against the number of interferers subtracted in the SIC strategy. The result corresponds to the case when rank of the link $R=2$. The solid line is the average result, and the dashed lines correspond to the average plus or minus the standard deviation of results.

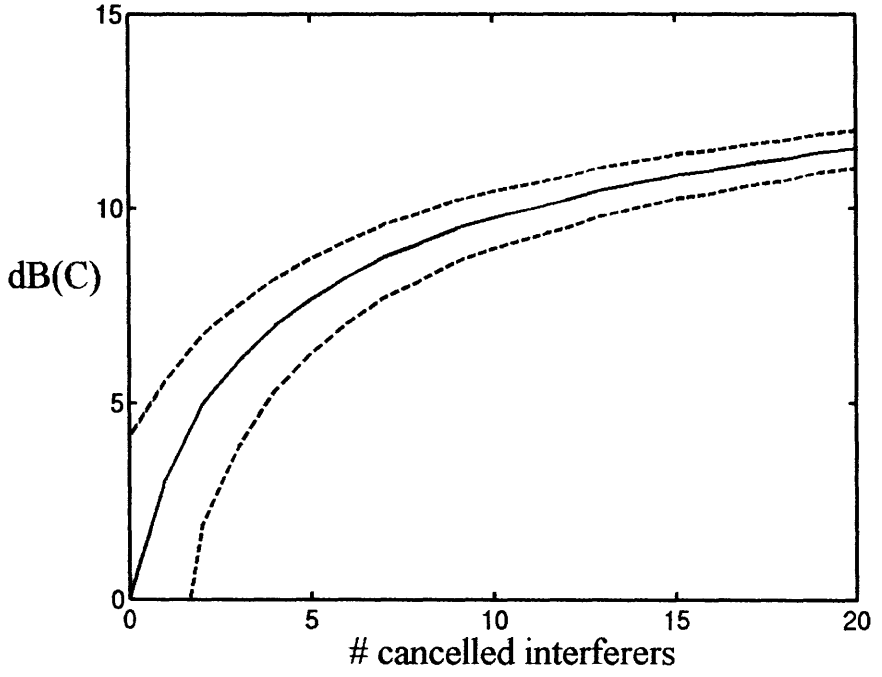

Figure 7: Improvement in dB of link capacity as defined in (19), plotted against the number of interferers subtracted in the SIC strategy. The result corresponds to the case when rank of the link R=3. The solid line is the average result, and the dashed lines correspond to the average plus or minus the standard deviation of results.

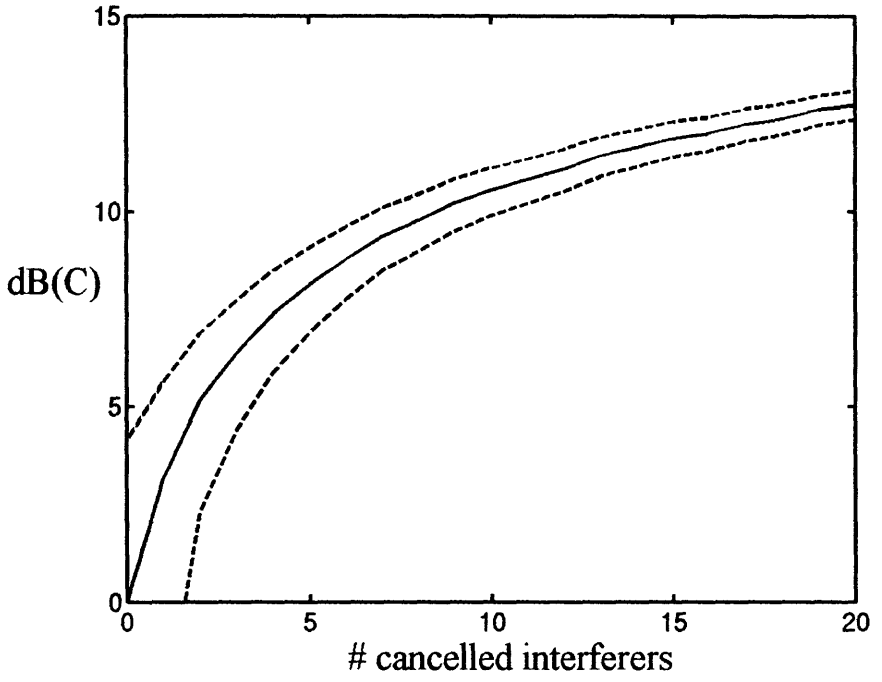

Figure 8: Improvement in dB of link capacity as defined in (19), plotted against the number of interferers subtracted in the SIC strategy. The result corresponds to the case when rank of the link R=5. The solid line is the average result, and the dashed lines correspond to the average plus or minus the standard deviation of results.

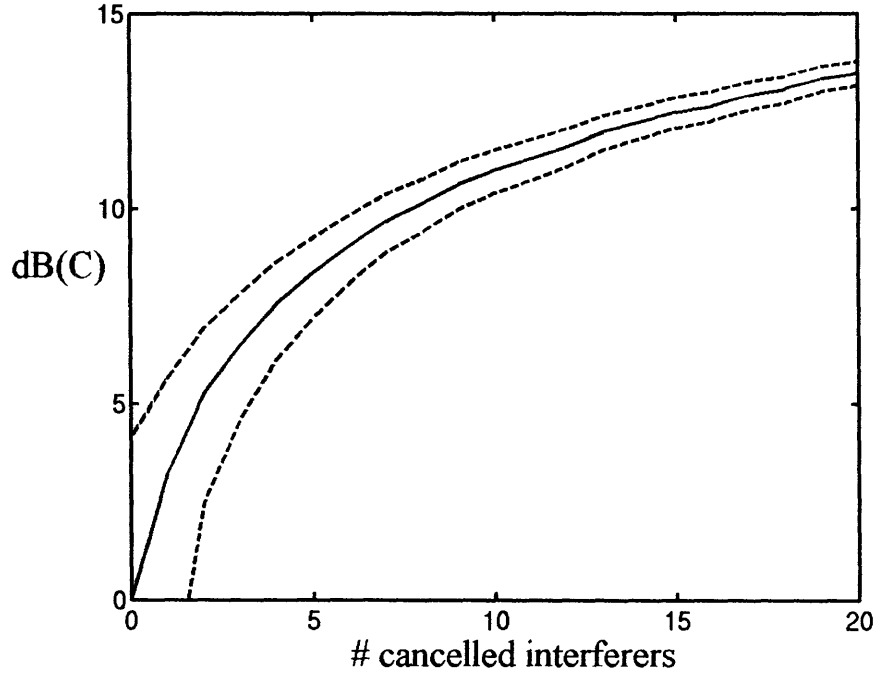

Figure 9: Improvement in dB of link capacity as defined in (19), plotted against the number of interferers subtracted in the SIC strategy. The result corresponds to the case when rank of the link R=10. The solid line is the average result, and the dashed lines correspond to the average plus or minus the standard deviation of results.

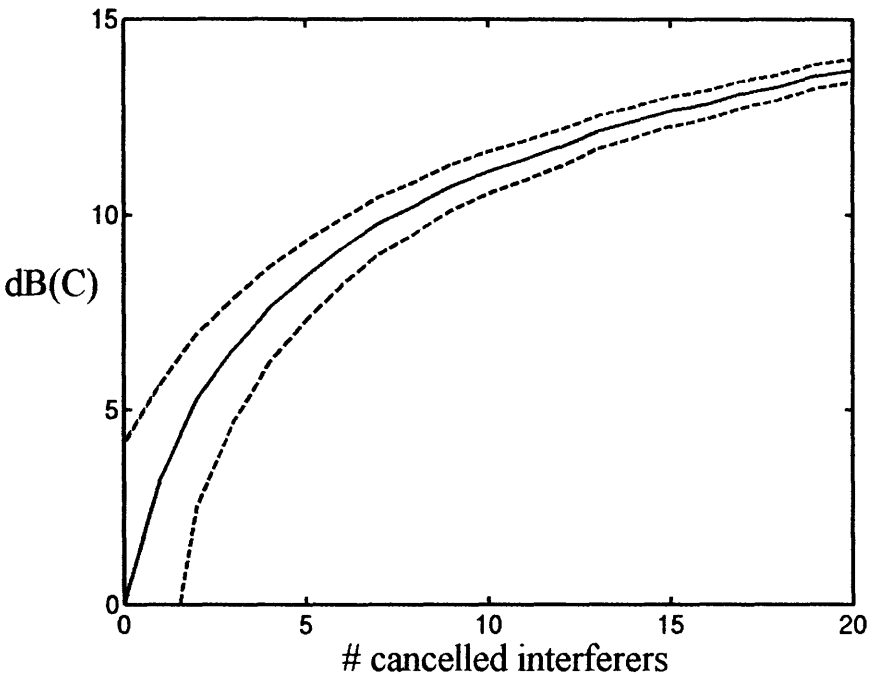

Figure 10: Improvement in dB of link capacity as defined in (19), plotted against the number of interferers subtracted in the SIC strategy. The result corresponds to the case when rank of the link R=20. The solid line is the average result, and the dashed lines correspond to the average plus or minus the standard deviation of results.

All these results are combined in the same plot in Figure 11, where one can see how the improvement curves shift upwards when R changes. The solid curves on the graph are all below the dashed line, and they correspond to the Shannon capacity from formula (19). The lowest of them is the result for $R = 2$, and as R increases, the improvement curves shift upwards. The dashed curve corresponds to the capacity defined by (20), and we can see that the solid curve for $R = 20$ lies almost at the same level as the dashed curve. That tells us that for high values of R the capacity improvement curves are the same for the two capacity definitions.

One can see that the greatest discrepancy of the improvements for two different capacities exists for $R = 2$ (see Figure 11), where the difference between the two curves is around $3.5dB$ for 20 subtracted interferers. This means that the gap between the Shannon limit and the achievable capacity (from formula (20)) decreases. The original gap, as noted in chapter 3, was around $6.2dB$ for $R = 2$, and for 20 subtracted interferers we can see that this gap can be reduced to less than half of its original value if you eliminate 20 closest interferers.

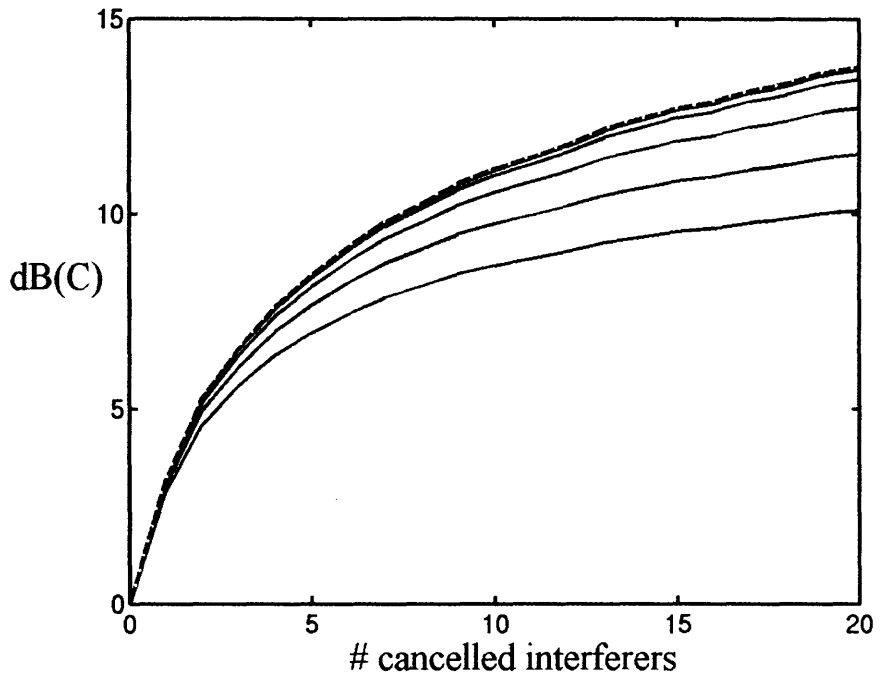

Figure 11: Improvement in dB of link capacity vs. number of interferers subtracted in the SIC strategy. The solid curves correspond the Shannon's capacity defined in (19), and they are plotted for the rank values, from bottom to top: *R=2, 3, 5, 10, 20.* The dashed curve on top corresponds to the improvement of the capacity defined in (20).

These plots achieve the goal of this chapter to present what happens with the link capacity when one uses the SIC strategy for enhancing the performance of the system. The plots of capacity improvement can be compared to the plots achieved with the multiple antenna system that is described in the following chapter, and the tradeoffs between the two strategies then become clear.

Chapter 4:

Multiple Antennas

4.1. Motivation

The link capacity that we looked at until now was derived for single antennas at each user, with equal antenna gain in all directions. This is not very practical since that way the receivers suffer interference coming from all directions, and the transmitters waste their power by transmitting with equal intensity in all directions instead of concentrating on the direction where the target receiver is located. As a consequence, a suboptimal *SINR* is achieved at the receiver's end of the link, and link capacity, which depends on the *SINR*, also stays at levels that are lower than in the case of appropriately designed non-isotropic antennas. The goal of this chapter is to examine what is the difference in the performance of the system when appropriately designed non-isotropic antennas are used.

In order to enhance the performance of the system, one should use directional antennas, with the lobes of the antenna gain pattern pointing towards the corresponding receiver or transmitter. There are many types of directional antennas, as described in [22], but in this thesis I use multiantenna arrays, which in effect can have a gain pattern same as directional antennas, just as long as correct multipliers are applied to each individual antenna in the antenna array. The difference between a directional antenna and a multiantenna array used in this thesis is in the fact that arrays consist of multiple individual isotropic dipole antennas. These isotropic dipole antennas are then multiplied by a complex vector, which corresponds to amplitude and phase shifts, and the sum of the multiplied signals is equal to the input signal in the multiantenna system. This way one can create a wide variety of antenna gain patterns, with lobes and nulls in optional directions. One is only limited by the number of peaks and nulls that can be placed in desired directions, since the number of degrees of freedom is limited by the number of dipole antennas in the array.

The reason for studying the effects of multiantenna arrays in this thesis lies in possible practical implementations of the system. Isotropic dipole antennas are simple to build and connect together. Also, after the array is built, one does not have to physically rotate the array in order to position a lobe in the desired direction, or place a null on an interferer, but instead, one just needs to find the optimal complex vector of multipliers, while the array stays physically in the same place. That would not be the case with some basic types of directional antennas, which is an advantage of multiantenna arrays over such directional antennas.

The array of isotropic antennas can, further, be attached to edges of a device, such as a laptop computer, which is a very likely candidate for a typical user in the wireless network we are trying to design. Later in the chapter I discuss what is the minimum spacing between the antennas in the antenna array, and the result that I got was $\frac{1}{2}\lambda$, where λ is the wavelength of transmitted signal. The bands that are likely to be reserved for wireless ad hoc networks are probably either going to be around $2GHz$ or $5GHz$. For these frequencies, the corresponding wavelengths are equal to:

$$\lambda = \frac{3 \cdot 10^8 \, m/s}{2 \cdot 10^9 \, Hz} = 0.15m, \tag{21}$$

and

$$\lambda = \frac{3 \cdot 10^8 \, m/s}{5 \cdot 10^9 \, Hz} = 0.06m. \tag{22}$$

From here we see that the minimum distances are $7.5cm$ and $3cm$, which means that the dipole antennas of the array can be attached to edges of a laptop, or an even smaller device. In conclusion, multiantenna arrays are likely to be easily implemented in wireless ad hoc networks. In this thesis, I concentrate on the performance of multiple antennas in simulation-oriented experiments under specific conditions.

4.2. Assumptions

Most of the conditions under which the formulas (19) and (20) were derived are valid in this chapter as well. All receivers and transmitters are randomly and uniformly

distributed in a plane with equal density $\left[\frac{\#users}{m^2}\right]$ and paired up in data communication links consisting of one receiver and one transmitter. All transmitters that are not in the link are considered to be interferers at the receiver of that link, and thermal noise of the receiver is considered to be negligible compared to the interference level at the receiver.

The difference from chapter 2 is in the fact that instead of one dipole isotropic antenna, users now have n isotropic dipole antennas arranged in an array ($n \geq 2$). All n antennas of a user are positioned in the plane of the network, vertically oriented, perpendicular to the plane and with isotropic individual gains in the plane. However, these antennas in combination have a non-isotropic gain pattern, with lobes and nulls in different directions, which depend on the complex multiplier vector with which the individual antenna signals are multiplied (vector $\vec{w}$ from equation (25)).

Transmitting and receiving users can both have multiantenna arrays, but in this thesis they have slightly different strategies. While a transmitter only tries to put maximum gain on the corresponding receiver, a receiver tries to both put a high gain on the corresponding transmitter and null its strongest interferers. It is important to notice that the communication approach in this chapter is not strictly speaking MIMO, although this kind of communication could be considered MIMO, since both transmitters and receivers have multiple antennas. Instead of looking at communication between multiple transmitting antennas and multiple receiving antennas all at once (MIMO approach), this chapter examines what happens separately at the receiving and transmitting end of the link, and distinguishes the contributions of the two to the link capacity.

Receivers

The receiving end of the link receives signals from many transmitters in its surroundings that act as interferers, as well as the desired transmitter from the other end of the link. The signal coming from a transmitter to the n receiving antennas is represented by a vector $\vec{z}$, whose entries are the received signals at individual antennas:

$$\vec{z} = \vec{v}\, s, \tag{23}$$

or else

$$\begin{bmatrix} z^1 \\ \vdots \\ z^n \end{bmatrix} = \begin{bmatrix} v^1 \\ \vdots \\ v^n \end{bmatrix} s, \tag{24}$$

where s is the signal being sent by the transmitter, $z^1,\ldots,z^n$ are signals in antennas $1,\ldots,n$, respectively, and $\vec{v}$ is the vector of the path loss coefficients. All variables in equation (24) have complex values, because they represent both power and phase of the signal and path loss. One can also imagine $z^1,\ldots,z^n$ and s as phasors in a complex plane, all having the same frequency, since they come from the same transmitter.

The signal that enters the *SINR* expression is then equal to the linear combination of signals at individual antennas $\vec{z}$:

$$s' = \vec{w}^H \vec{z}, \tag{25}$$

where $\vec{w}$ is the weight vector, of complex values w_i :

$$\vec{w} = \begin{bmatrix} w_1 \\ \vdots \\ w_n \end{bmatrix}, \tag{26}$$

and $\vec{w}^H$ is its complex conjugate.

The equations (23)-(26) describe the received signal s' no matter if the signal s originates at the desired transmitter or at an interferer. The only difference is in its place in the expression for *SINR*. Since this thesis neglects the thermal noise of the receiver, the expression for *SINR* is:

$$SINR = \frac{s's'^H}{\sum_i s_i' \, s_i'^H}, \tag{27}$$

where s^H and s'^H are complex conjugates of s and s', respectively, $s's'^H$ is the power of the desired signal, $s_i' \, s_i'^H$ is the power of an interferer, and the summation is performed over all interferers i in the network. Note that the interfering signals are considered to be

independent and that is why one can simply add their individual powers in order to get the total interference power.

The goal of the receiver is to maximize the *SINR*, which maximizes the capacity of the link (see (8) and (9)), and the way to maximize *SINR* is through adjusting the weight vector $\vec{w}$ in the following expression, which can be derived from (23), (25), and (27):

$$SINR = \frac{\vec{w}^H \vec{v}\ s\ s^H \vec{v}^H \vec{w}}{\sum_i \vec{w}^H \vec{v}_i\ s_i\ s_i^H \vec{v}_i^H \vec{w}} \tag{28}$$

where the values for $s, s_i, \vec{v}$ and $\vec{v}_i$ are all given by the network setup, while the receiver can adjust $\vec{w}$ in order to maximize the *SINR*. Since one of the assumptions of this thesis is that all transmitters radiate equal power, the values $s\,s^H$ and $s_i\ s_i^H$ are equal and they cancel each other out from equation (28). The final expression is then:

$$SINR = \frac{\left(\vec{w}^H \vec{v}\right)\left(\vec{w}^H \vec{v}\right)^H}{\sum_i \left(\vec{w}^H \vec{v}_i\right)\left(\vec{w}^H \vec{v}_i\right)^H}. \tag{29}$$

One can use different methods to maximize expression (29). This thesis performs gradient search for the optimum $\vec{w}$ vector, and later parts of this chapter describe the procedure. One can also use MMSE and MVDR methods described in [23]. Since there is a unique solution to this problem, the method used should not really matter, because all of them should lead to the same solution under the same network setup conditions. However, the way you choose $\vec{v}$ and $\vec{v}_i$ is a very sensitive issue, since the resulting $\vec{w}$ and *SINR* very much depend on these values.

The main issue is how to calculate the phase difference of the path loss, $\vec{v}$ and $\vec{v}_i$, because the power difference is already determined by (1) and (10). The phase difference of each coefficient in $\vec{v}$ and $\vec{v}_i$ depends on all diffractions and reflections that happen during the propagation along various paths from the transmitter to the antenna in the receiver's antenna array, which is very complicated to estimate. In order to avoid complicated models and estimations of the complete path loss, including the phase

difference, this chapter considers two models that are both extreme cases and antipodes to one another.

Line of Sight

The first model is line of sight (LOS). Instead of having multiple paths along which the signal travels from the transmitter to the receiving antenna, with diffractions and reflections along those paths, there is only one such path, and that is a straight line. In this case the phase difference of the path loss depends on the distance between the transmitter and the receiving antenna, and in combination with the equation (10), we get the formula for the entries of vectors $\vec{v}$ and $\vec{v}_i$:

$$v^j = \left(\frac{r}{r_0}\right)^{-\alpha/2} \cdot e^{i\frac{2\pi}{\lambda}r}, \tag{30}$$

where v^j is the path loss coefficient from the transmitter to the j^{th} receiving antenna, r is the distance between them, and λ is the wavelength of the transmitter signal. These values of v^j coefficients imply received signal power proportional to $r^{-\alpha}$.

When distances between the antennas in the array of receiving antennas are much shorter than the distance to the transmitter, r, then the right hand side of (30) can be divided into the magnitude part which depends only on r, and the phase part which depends only on the direction where the transmitter is located. This assumption is considered to hold in this chapter, and as a consequence, the path loss vector depends on the direction of the transmitter in the following way:

$$\vec{v} = r^{-\alpha/2} \cdot \vec{f}(\vartheta), \tag{31}$$

where ϑ is the angle of the direction of the transmitter ($0 \le \vartheta \le 2\pi$), and the function $\vec{f}(\vartheta)$ does not depend on r. The same equation (31) is also valid for $\vec{v}_i$.

The experiment with receiving multiantennas is described later in the chapter, and one of its initial steps was calculating the values of $\vec{f}(\vartheta)$ for all transmitters in the network.

One important thing to notice is that values of $\vec{f}(\vartheta)$ coefficients depend on the spacing between the antennas of the array. For small spacing (less than $\lambda/2$), these

coefficients are very close to each other and, as a consequence, the signal becomes buried in the noise. This effect is studied at the end of this chapter.

Extreme Multipath

In contrast to the LOS case where there is only a single, line of sight, path for the signal to come to the receiver, in the extreme multipath (EM) case, there are many paths, and the total path loss is determined by the sum of all individual path losses. This model assumes a great number of individual paths, with all kinds of individual phase and power differences, and as a consequence, their sum is considered to be a random variable.

The resulting phasor of the sum of phasors from each of the multiple paths between the transmitter and the receiving antenna is under the EM assumption modeled as a complex Gaussian random variable. The amplitude of that random variable is Rayleigh distributed and the square of the amplitude is exponentially distributed with mean $(r/r_0)^{-\alpha}$, while its phase is a uniform random variable: $0 \le \varphi \le 2\pi$. The corresponding $\vec{v}$ vector is equal to:

$$\vec{v} = \begin{bmatrix} v^1 \\ \vdots \\ v^n \end{bmatrix}, \tag{32}$$

where $v^1, \ldots, v^n$ is a set of independent complex Gaussian random variables with variance equal to $(r/r_0)^{-\alpha}$. Phases of the coefficients v^j are randomly and independently chosen from the uniform distribution $0 \le \varphi \le 2\pi$. The same formula (32) is also valid for $\vec{v}_i$.

One can see from (31) and (32) that the main difference between LOS and EM is in the way the $\vec{v}$ coefficients are chosen. In the LOS case, the coefficients are completely deterministic and interdependent, and also dependent on the angle ϑ of the transmitter direction. One the other hand, in the EM case, the coefficients $\vec{v}$ are random and independent from each other. The two cases present two extremes, and since the realistic case is bounded by these two cases, the experiments described later in the chapter give not only the results for LOS and EM, but also bounds for the cases that are in between of these two extremes.

Transmitters

When the transmitter has an array of multiple antennas, it is less complicated to determine that effect on the link capacity than in the case when the receiver has multiple antennas. This is because of the difference in the usage of those antennas. While the receiver is likely to try to both place a high gain on the desired transmitter and null the closest interferers, all by adjusting the weight vector $\vec{w}$ on the antenna array in order to get the maximum *SINR*, the transmitter is normally only concerned with putting a high gain on its receiver.

Since this chapter examines separately the effects of multiple antennas at the receiver and transmitter's ends of the link, for the case when the transmitter has multiple antennas, the receiver is considered to have a single receiving antenna. Under this condition, there are n signals at the receiver, coming from n transmitting antennas. These signals add together and their sum is equal to the effective signal at the receiver. The transmitter then adjusts the weight vector $\vec{w}$ on the transmitting antennas in order to get the maximum signal at the receiver.

One can calculate the maximum possible gain that the n antennas produce by finding the most constructive sum of the n separate signals at the receiver. These signals can be represented as phasors, and their sum is the sum of their phasors, and the most constructive sum of the phasors occurs when they are collinear. In that case the amplitude of the sum of the n signals is the maximum amplitude, and it is equal to n times the amplitude coming from one transmitting antenna.

That means that the effect of having n antennas at the transmitter's end increases the signal power by a factor of n^2. However, the effect of multiple transmitting antennas on the overall level of interference in the network is also multiplicative. If all transmitters have n antennas, then the aggregate power they emit is n times stronger than the power they emit when each of them has only a single antenna. Since the numerator of the expression for *SINR* increases by a factor of n^2, and the denominator by a factor of n, in the end the effect of having n antennas at the transmitting end of each link increases *SINR* by a factor of n.

This thesis does not explain the technique of finding the optimum weight vector $\vec{w}$ for the array of transmitting antennas, for which the link gets maximum *SINR* improvement. Instead of that, it only discusses the effect, the corresponding improvement of *SINR* and link capacity.

4.3. Capacity Improvement

This section presents the results of simulation-based experiments for measuring the link capacity improvement when the users in the network have multiple antenna arrays at hand. For the case when receivers had multiple antennas, experiments were performed in order to get the CDF values for capacity improvement over the single antenna case, while in the case of multiple transmitting antennas the plots of improvement presented the dB gain as a function of the number of antennas n.

Receivers

In the experiment for calculating improvement due to a multiantenna array at the receiver's end, there were 1000 trials of the experiment, which was used to get the CDF values for the dB improvement of the *SINR*. In one trial there was one receiver in the center of the network, and 1000 interferers were randomly and uniformly distributed in a square around the receiver. This number of interferers was enough to simulate an infinite plane of interferers, since the network outside the square would have a negligible contribution to the interference at the receiver in the center, which can be proven by using formula (15). The transmitter's position was randomly chosen at the edge of the square, which corresponds to very high values of rank R.

The expression (29) was used for maximizing *SINR*, where the values for $\vec{v}$ and $\vec{v}_i$ were determined by the network setup and the receiver could adjust the $\vec{w}$ vector in order to get the maximum improvement of *SINR*. There were two ways for calculating $\vec{v}$ and $\vec{v}_i$, one under the LOS assumption, by using (30) and (31), and the other under the EM assumption, by using (32).

Under the LOS assumption, the physical shape of the antenna array was important because the values for $\vec{v}$ and $\vec{v}_i$ depended on it. The experiments of this thesis explore the cases of 2,3, and 4 antennas, and, apart from the antenna spacing, only in the 3 and 4 antenna case was there freedom to choose the geometrical shape of the array. In this thesis, the 3 and 4 antennas were put in vertices of a square whose sides were equal to $\lambda/2$ In the 2 antenna case the antenna spacing was subject to change, and the results of the experiments showed that the *SINR* improvement did not depend on the antenna spacing. More explanations about this effect are in the later part of this chapter.

In order to maximize the expression (29) I used gradient search over the values of $\vec{w}$. For each maximization process, the program chose 100 random starting points in the space of possible values for $\vec{w}$, and conducted a gradient search. The space of possible values for $\vec{w}$ were all those vectors $\vec{w}$ whose coefficient satisfied the conditions $0 \le |w_j| \le 1$ and $0 \le phase(w_j) \le 2\pi$. The step size in the gradient search was equal to $\Delta = 0.05$.

Results

Since the *SINR* improvement was the consequence of using multiple antennas, the results of the described experiments entered the link capacity formulas (19) and (20) through the factor β. In Figures 12 and 13, the CDFs of the *dB* values of β are presented under two different assumptions, LOS and EM. These functions are later used to estimate the *dB* improvement of link capacities defined by (19) and (20).

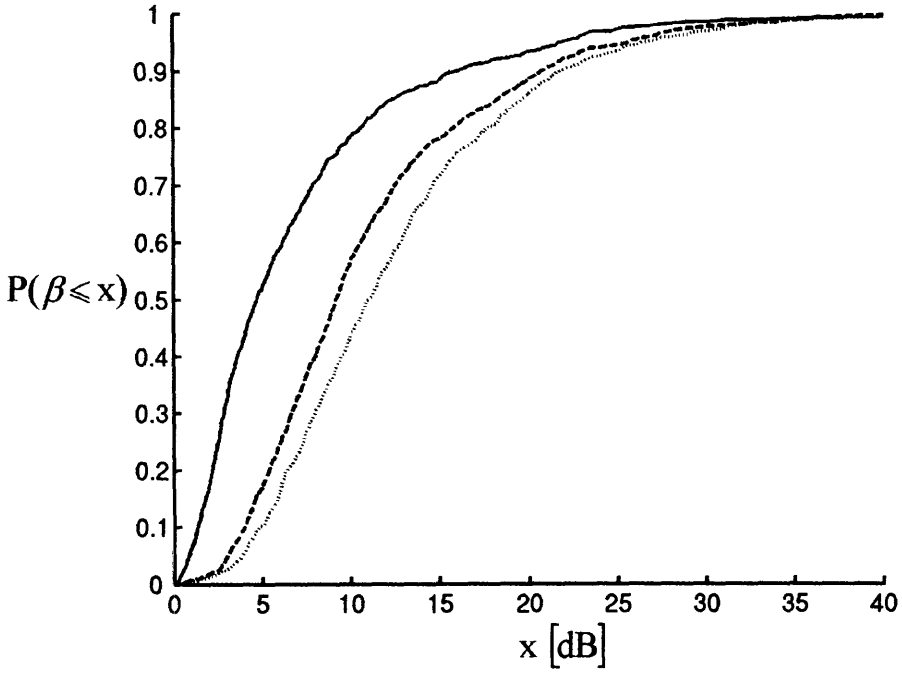

Figure 12: Experimental results for dB values of β under the EM assumption and for different numbers of receiving antennas. The leftmost (solid) curve is the CDF for the case of 2 antennas. The middle (dashed) curve is the CDF for the case of 3 antennas. The rightmost (dotted) curve is the CDF for the case of 4 antennas.

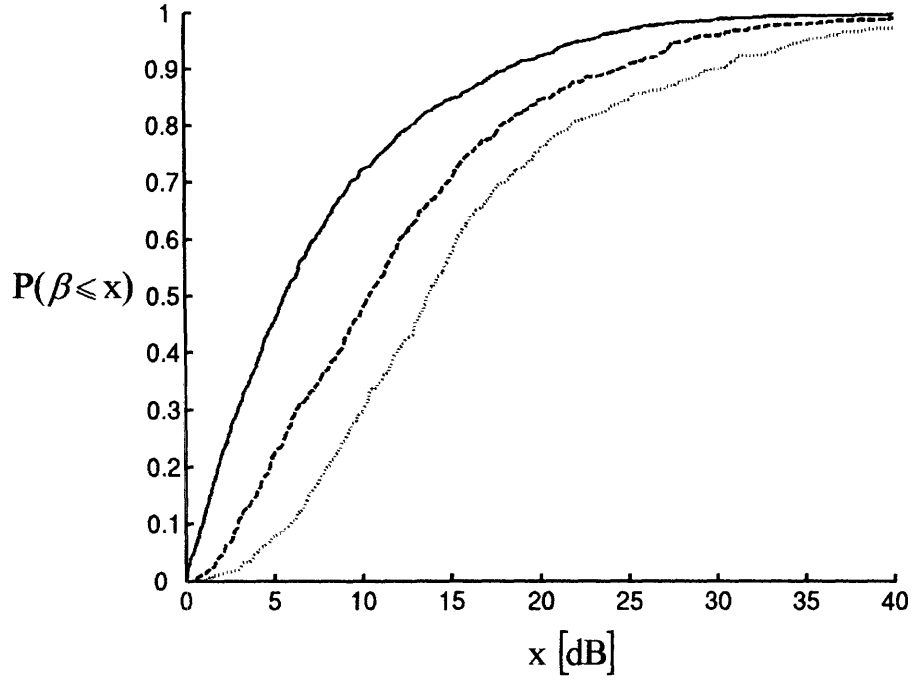

Figure 13: Experimental results for dB values of β under the LOS assumption and for different numbers of receiving antennas. The leftmost (solid) curve is the CDF for the case of 2 antennas. The middle (dashed) curve is the CDF for the case of 3 antennas. The rightmost (dotted) curve is the CDF for the case of 4 antennas.

The CDFs for β together with the formulas (19) and (20) give the corresponding outage link capacity improvements as functions of the number of antennas n. Each of the Figures 14-18 presents outage capacity improvements for 95%, 80%, 50%, and 20%, under both LOS and EM conditions. By definition, the 95% outage capacity improvement is the level of capacity improvement for which 95% of the links have capacity improvement greater than that level of improvement. Similar definitions are valid for 80%, 50%, and 20% outage capacity improvements.

Figure 14 shows the outage capacity improvements for β and link capacity as defined in (20), as a function of the number of receiving antennas n. These two functions are the same because the capacity from (20) is proportional to β. Figures 15-18 present outage capacity improvements for the link capacity defined in (19). The results presented in Figures 15-18 also depend on the rank R of the link, and one can see the tendency that these plots shift towards greater improvement as R grows. In the limit, these improvement curves approach the curves from Figure 14. One can see how for $R = 10$ the improvement curves from Figures 14 and 18 are very similar, while the curves for $R = 20$, which are not pictured here, are indistinguishable from the curves in Figure 14.

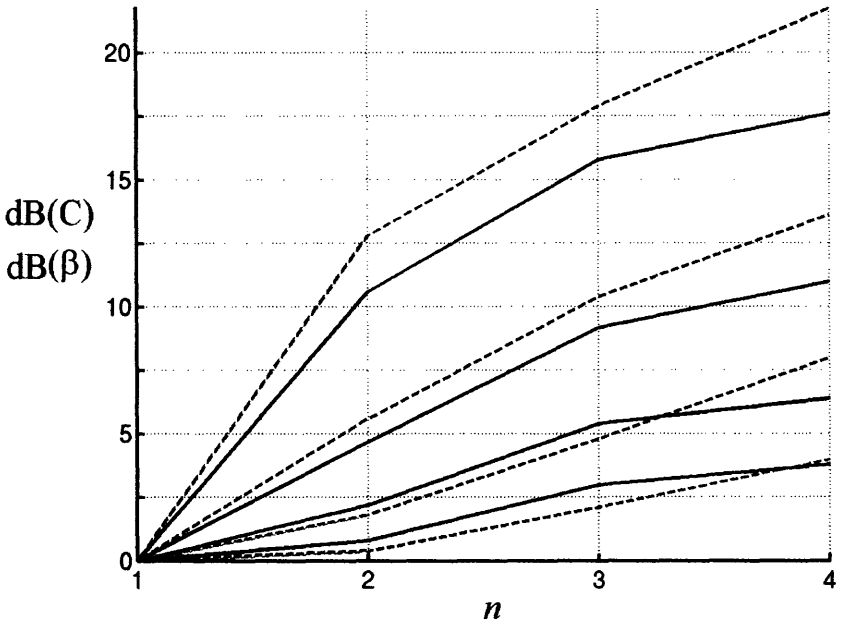

Figure 14: Outage capacity improvements for link capacity defined in (20), as a function of the number of receiving antennas n. The results are equal to the outage improvements of β. The dashed curves correspond to the results under the EM assumption, and the solid curves to the results under the LOS assumption. The pairs of solid and dashed curves from the bottom to the top, respectively, represent 95%, 80%, 50%, and 20% outage improvements.

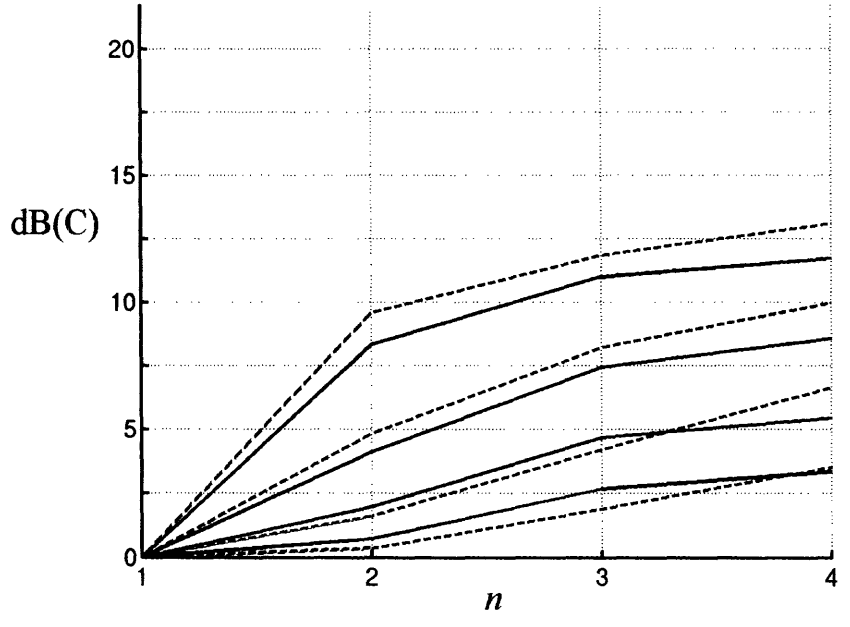

Figure 15: Outage capacity improvements for link capacity defined in (19), as a function of the number of receiving antennas n. The results represent the links of rank $R = 2$. The dashed curves correspond to the results under the EM assumption, and the solid curves to the results under the LOS assumption. The pairs of solid and dashed curves from the bottom to the top, respectively, represent 95%, 80%, 50%, and 20% outage improvements.

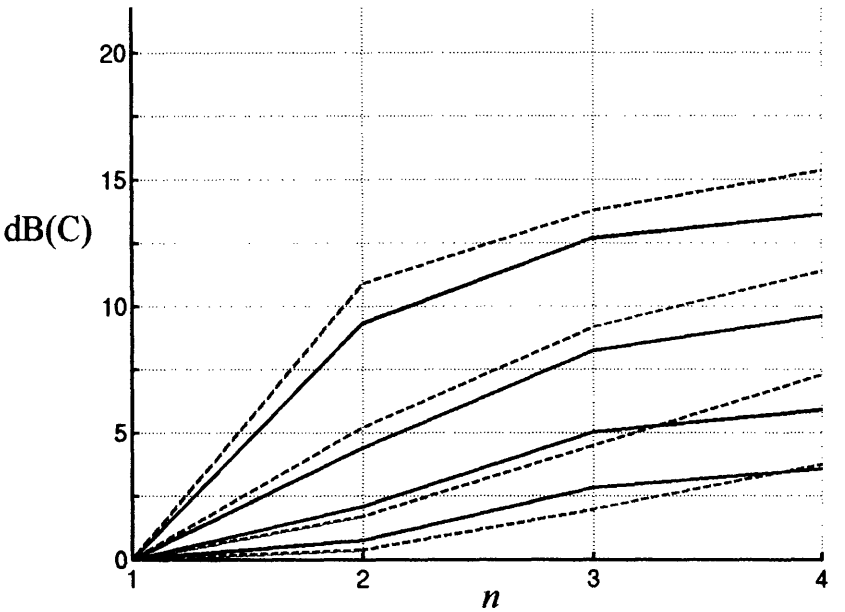

Figure 16: Outage capacity improvements for link capacity defined in (19), as a function of the number of receiving antennas n. The results represent the links of rank $R = 3$. The dashed curves correspond to the results under the EM assumption, and the solid curves to the results under the LOS assumption. The pairs of solid and dashed curves from the bottom to the top, respectively, represent 95%, 80%, 50%, and 20% outage improvements.

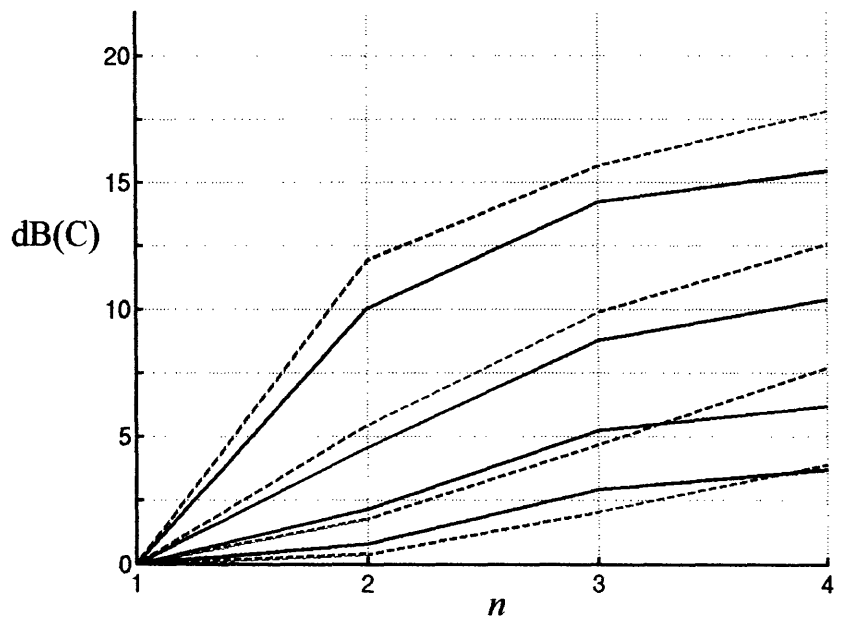

Figure 17: Outage capacity improvements for link capacity defined in (19), as a function of the number of receiving antennas n. The results represent the links of rank $R = 5$. The dashed curves correspond to the results under the EM assumption, and the solid curves to the results under the LOS assumption. The pairs of solid and dashed curves from the bottom to the top, respectively, represent 95%, 80%, 50%, and 20% outage improvements.

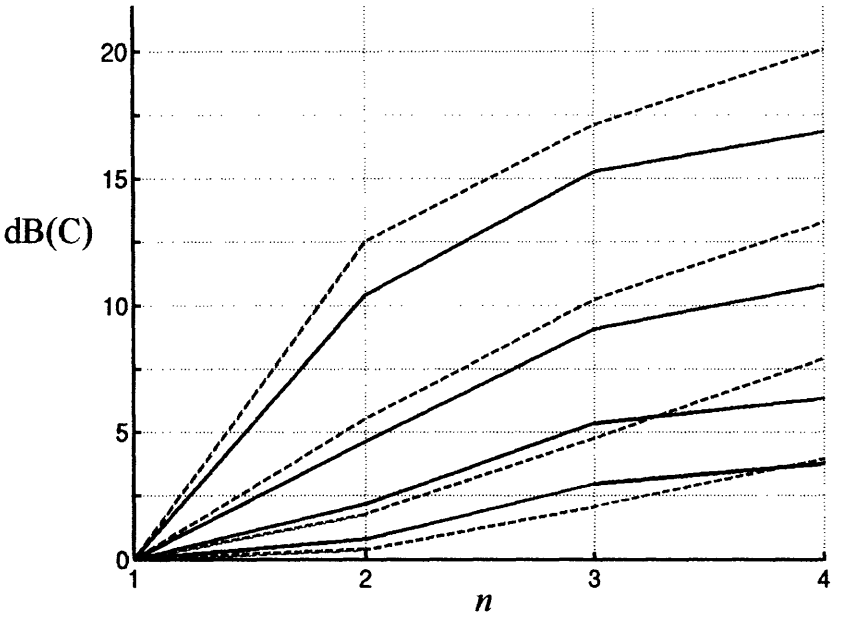

Figure 18: Outage capacity improvements for link capacity defined in (19), as a function of the number of receiving antennas n. The results represent the links of rank $R = 10$. The dashed curves correspond to the results under the EM assumption, and the solid curves to the results under the LOS assumption. The pairs of solid and dashed curves from the bottom to the top, respectively, represent 95%, 80%, 50%, and 20% outage improvements.

Transmitters

The benefit of multiple transmitting antennas on the link capacity was less than the benefit of multiple receiving antennas, which is a consequence of different usage of multiple antennas by receivers and transmitters, which was explained in the previous parts of this chapter. There was also a difference in the ways of measuring those effects. Since the receivers both try to peak up on the corresponding transmitter and decrease the influence of the interferers, there was a need to perform experiments in order to measure the effects of that strategy. On the other hand, the only chosen goal of the transmitters with multiple antennas was to put the maximum gain on the corresponding receiver, and that effect could be measured without simulations and experiments.

The analysis in a previous part of this chapter explains how the effect of having n antennas at the transmitting end of each link increases the signal power at the receiver by a factor of n^2, the interference level at the receiver by a factor of n, and the *SINR* over

the link by a factor of n. The conclusion of this analysis was that, when all network transmitters have n antennas and the receiver has a single antenna, the multiplier β from the equations (19) and (20) is equal to $\beta = n$. That result was derived under the assumption that there is a single receiving antenna, which is our model for examining the effect of multiantennas at the transmitter separately from multiantennas at the receiver.

Figure19 presents the dB values of β as a function of the number of antennas n, as well as the dB improvement of the link capacity defined by (20). These two functions are equal since the capacity from (20) is proportional to β. Figure 20 presents the dB improvement curves for the link capacity defined in (19), as a function of the number of antennas n. Different improvement curves correspond to different values of the link rank R. The bottom curve corresponds to the value $R = 2$, and the curves shift upwards as R grows. In the limit, for large R, these curves approach the curve from Figure 19.

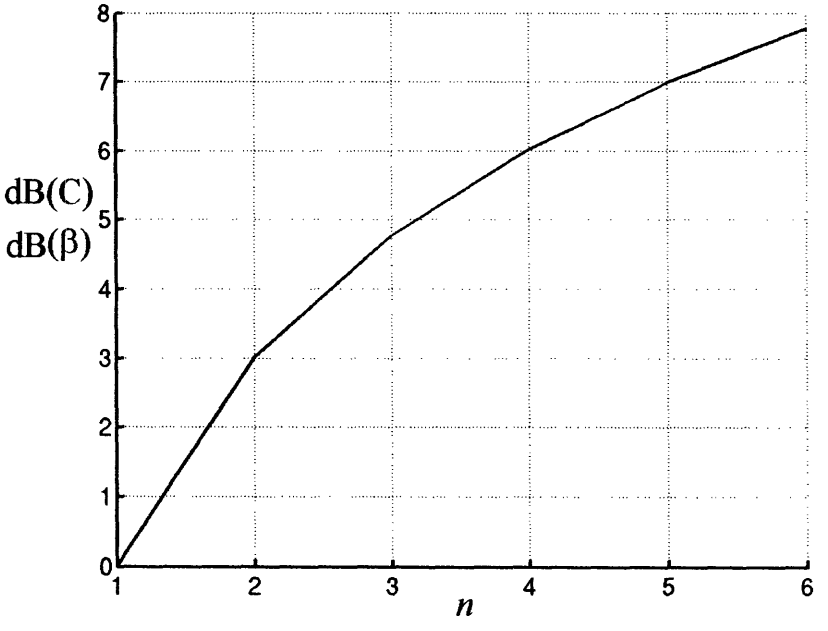

Figure 19: Improvement in dB of β and link capacity as defined in (20), plotted against the number of antennas at the transmitter.

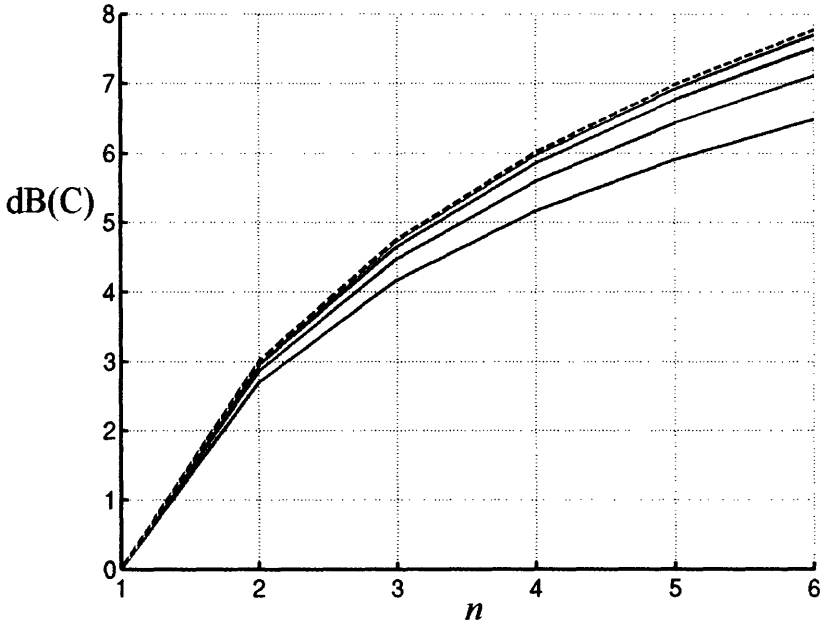

Figure 20: Improvement in dB of link capacity vs. number of antennas at the transmitter. The solid curves correspond Shannon's capacity defined in (19), and they are plotted for the rank values, from bottom to top: *R=2, 3, 5, 10, 20.* The dashed curve on top corresponds to the improvement of the capacity defined in (20).

4.4. Single User Exception

In the analysis for multiple transmitting antennas, the assumption was that all transmitters in the network had the same number of antennas. However, the case when a single transmitter has a different number of antennas may also arise. There are two representative cases, one when all transmitters have n antennas except for one that has 1 antenna, and the other when all transmitters have 1 antenna except for one that has n antennas.

In the first case the interference level at the receiver that is paired up with the single-antenna transmitter is the same as for all other receivers in the network, while the signal coming to the receiver is n^2 times weaker than for other links of similar length. In conclusion, the loss in the *SINR* is n^2, and the loss of the link capacity is double the improvement curves from Figures 20 and 21, but with negative sign in front of it. Other

users on average have the same link capacities as if there was no exceptional user in the network.

In the second case, all transmitters have a single antenna, except for one that has n antennas. The average interference level in that case is equal for all because the interference level is equal to aggregate interference coming from all transmitters in the network, and the single exceptional transmitter does not significantly change the overall interference in the network. On the other hand, the signal power at the receiver of the exceptional link is n^2 times stronger than for other links of the similar length. As a consequence, the SINR of the exceptional link is n^2 times stronger than for similar links in the network. The corresponding improvement of link capacity in dB for the exceptional user is double the improvement curves in Figures 19 and 20. Other users on average have the same link capacities as if there was no exceptional user in the network.

The effect of a receiver having different number of antennas from the other receivers in the network is not as strong as for the transmitters. Since other receivers do not contribute to the interference level or have any other direct influence over the *SINR* level at the exceptional receiver, the dependence of the capacity of the exceptional link on the number of antennas at the receiver is the same as what was represented in Figures 14-18.

4.5. Antenna Array Spacing

One of the issues in the system design is the spacing between the antennas of the antenna arrays. It is very important to know if there are any limiting factors for the array spacing, because the practical implementation of the system depends on them.

The experiment that discovers the limiting factor for the array spacing was performed under the LOS assumption. The other assumption, extreme multipath, was not used since the author learned in a conversation with Daniel Bliss that the field experiments show that the EM model is poor when the distance between the antennas is smaller than approximately one wavelength λ

Under the LOS assumption, which is more interesting for close antenna spacing, the experiments with two-antenna receiving arrays show the following results. For the two-antenna case, the overall maximum *SINR* improvement does not change as the distance between the two receiving antennas shrinks. This improvement is equal to the improvement of β and fixed-bit-error-rate capacity (from (20)) improvement and those values are plotted in Figure 21. However, even though the maximum link capacity does not change when the antenna spacing decreases, both the received signal power W_{signal} and the interference power W_{interf} decrease dramatically when the distance between the antennas goes below $\lambda/5$ (see Figure 21).

The problem with low signal and interference power level is with the assumption of neglecting the thermal noise. If we assume negligible thermal noise, then we can derive the simple-form capacity expressions (19) and (20), as well as make the plots for capacity improvement from this chapter and the previous chapter.

However, if the signal and interference powers drop as dramatically as in Figure 21 for low values of d, then not only the results from this thesis are invalid because of non-negligible thermal noise, but also the signal might become buried in the noise and the receiver might not be able to recover it at all. That is why the antenna spacing needs to be limited. These results suggest the condition $d \geq \lambda/2$ in order to have a well-behaved system.

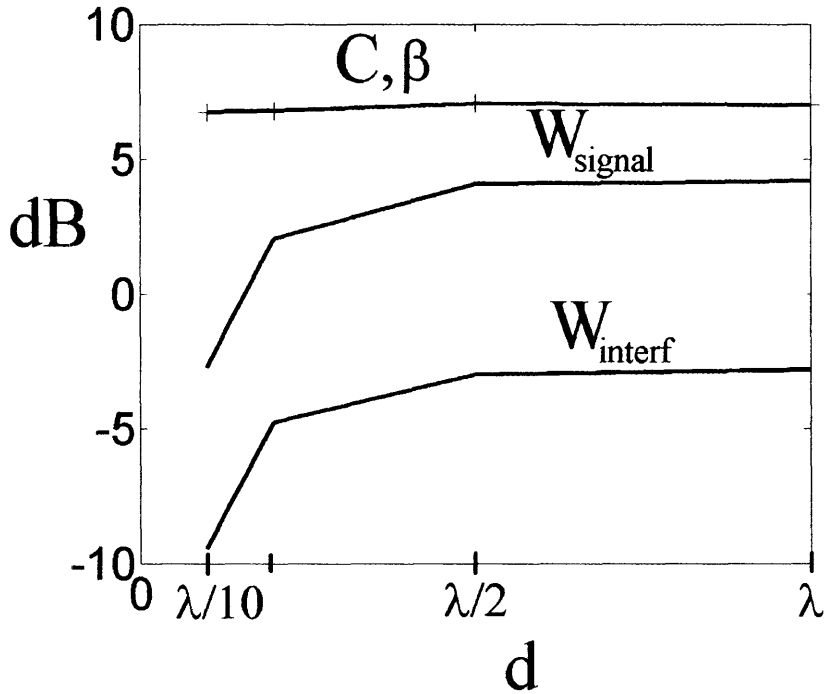

Figure 21: The top plot represents the dB improvement of β and link capacity C as defined in (20) when the receiver has an array of 2 antennas in the LOS environment, as a function of the spacing d between the two antennas. The middle plot represents the dB change of the signal power W_{signal}, as a function of d. The bottom plot represents the dB change of the interference power W_{interf}, as a function of d. Distance d is described in terms of the transmission wavelength λ.

Chapter 5:

Optimal Spatial Reuse

5.1. Overview

The previous chapters defined link capacity and presented how it depended on various design components of the system, such as the SIC strategy and application of multiple antennas. However, none of the described strategies cared whether spatial reuse was on the optimal level, and, in fact, none of them had means to adjust the level of spatial reuse.

The basic concept of spatial reuse means that the users that are far away and have no intention to communicate with each other can use the same frequency channel as long as they are far enough apart. However, if they are too far apart, then the bandwidth gets wasted, since more users could be packed in the same channel. At the same time, it is not good either to make the channel crowded with users, since then the interference level in individual communication links might become very large. In conclusion, one needs to find the correct number of channels for the network, so as to reach maximum satisfaction of the users.

The best satisfaction, as stated in chapter 2, occurs when the data rates over the links are the highest. In this chapter, the data rates are going to be calculated according to formulas (8) and (9), which represent Shannon's capacity and data rates with fixed tolerable bit error rate and modulation scheme for links in the wireless ad hoc networks considered in this thesis.

One of the basic network setup elements in the previous chapters was that all users were sharing the same frequency channel. However, that might not be the perfect setup. Users might get greater data rates if they divide the bandwidth into equally sized frequency subchannels, and randomly occupy those subchannels.

It is clear that those subchannels will have different level of spatial reuse, since the density of users in each of the subchannels is less than in the original single channel. The spatial reuse level can be measured by the network parameter, *NP*, which is an index value that characterizes the saturation of the network subchannel with users, and is defined in chapter 2. When the original channel is split into the subchannels, then the *NP* decreases, since the density of the users in the same frequency band decreases, and later parts of this chapter determine the optimal level of *NP* for which the individual link capacities are maximized.

The author acknowledges the contribution of Siddhartan Govindasamy in developing the ideas and deriving the results of this chapter.

5.2. Problem Definition

The model of wireless ad hoc network that was described in chapter 2 and used in the rest of the thesis is also used in this chapter. Such network consists of equal number of transmitters and receivers, distributed randomly and uniformly in a plane with densities ρ [$\#transmitters/m^2 = \#receivers/m^2 = \#users/m^2$]. Each receiver is linked to a transmitter from the network, and all other transmitters are considered to be interferers for the communication over that link. All links have their rank, which is an index value defined in chapter 2, and one can calculate the data rate over the link as a function of rank for $R \geq 2$ by using formulas (19) and (20). The path loss model is polynomial, with attenuation constant $\alpha = 3.8$, and thermal noise is considered to be negligible in comparison to the total interference level at the receiver.

The difference between the previous network model and the model in this chapter is in the usage of the frequency bandwidth $B[Hz]$ available to the network. Previously, the whole frequency bandwidth was one channel, and all users occupied that single channel, thus, maximally interfering with each other. In this chapter, the total bandwidth B is, instead, divided into N subchannels, whose individual bandwidths are B/N. All users are also divided into N equal subsets, each subset occupying one of the N subchannels. The assumption is that the users are randomly assigned to different

subchannels, which makes the density of users in each of the subchannels on average N times smaller than the overall density of the users in the network:

$$\rho = \frac{\rho_0}{N}, \tag{33}$$

where ρ is the density of users in one of the N subchannels, and ρ_0 is the overall density of users in the network. Note that the density of users in this thesis is equal to the density of transmitters and the density of receivers, individually, as opposed to being equal to their sum.

Links are assumed to belong to one subchannel, which means that the receiver and the transmitter from the link belong to the same subchannel. Link length always stays the same, and as a consequence, the network parameter corresponding to the link changes its value when the original frequency channel is divided into subchannels. The dependence of the network parameter on the number of subchannels is derived in the following equations, after plugging in the equation (33) into the network parameter definition (6):

$$NP = r \cdot \sqrt{\frac{\rho_0}{N}}$$

$$NP = \sqrt{\frac{R}{\pi \rho_0}} \cdot \sqrt{\frac{\rho_0}{N}}$$

$$NP = \sqrt{\frac{R}{\pi \cdot N}}, \tag{34}$$

where r is the link length, R is its original rank in the network, before dividing the network into subchannels, and ρ_0 is the overall density of users in the network.

The goal of this chapter is to find the optimal number of subchannels N for maximum data rate over the links in the network, and also to find the corresponding optimal value for NP (34) in the subchannel networks after the division. In order to find a unique solution for NP, it is assumed that all links in the original network have the same rank R.

For finding the maximum data rate over the link, one can use link capacity formulas (8) and (9), and multiply them with the subchannel bandwidth B/N, but *SINR* also needs to be calculated. One of the results of chapter 2 was that the interference level at the receiver was proportional to the density of the users to the power of $\alpha/2$. As a consequence, the following relation holds:

$$SINR = SINR_0 \cdot \left(\frac{\rho_0}{\rho}\right)^{\alpha/2}, \tag{35}$$

where *SINR* is the signal-to-interference-and-noise ratio on the link in the subchannel, $SINR_0$ is the signal to interference and noise ratio in the original channel, ρ_0 is the overall density of users in the network, ρ is the density of users in one of the N subchannels. The formula holds only when there is no discrepancy that occurs when the transmitter of the link is absent from the sum of uniformly distributed interferers.

Multiplier $\delta(R)$ in chapter 2 modeled this discrepancy. However, in this chapter, the values of *NP* and rank in the subchannel network suggest that this discrepancy has no effect and that formula (35) is valid. This is because the resulting values of *NP* from 0.35 to 0.65 that are derived in the following section of the chapter suggest that all interferers whose distance to the receiver is less than $2r$ are excluded from the subchannel, where r is the link length. That implies that all discrepancies coming from the absence of one transmitter from total sum of interferers are also excluded from the subchannel, and the subchannel network has uniformly distributed interferers.

As a consequence, the value of $SINR_0$ in formula (35) should be calculated without the $\delta(R)$ multiplier:

$$SINR_0 = \gamma \cdot \beta \cdot R^{-\alpha/2}, \tag{36}$$

where R is the rank of the link in the original network ($R \geq 2$), $\gamma = 0.5473$, β is the improvement of SINR due to the application of SIC or multiple antennas.

After plugging in the formulas (33) and (36) into (35), the expression for *SINR* becomes:

$$SINR = \gamma \cdot \beta \cdot R^{-\alpha/2} \cdot N^{\alpha/2}, \tag{37}$$

and this value can be plugged in into the formulas (8) and (9) in order to get the link capacities:

$$C = \log_2\left(1 + \gamma \cdot \beta \cdot R^{-\alpha/2} \cdot N^{\alpha/2}\right)\left[\frac{\#bits}{\sec \cdot Hz}\right], \tag{38}$$

which corresponds to Shannon's limit of the link capacity, and

$$C = \gamma \cdot \beta \cdot R^{-\alpha/2} \cdot N^{\alpha/2} \cdot \frac{1}{E_b/N_0}\left[\frac{\#bits}{\sec \cdot Hz}\right], \tag{39}$$

which corresponds to the bit rate under a fixed value for E_b/N_0 .

Data rate of the link is equal to the link capacity of that link multiplied by the bandwidth of the subchannel. In this case, the corresponding bit rates are equal to:

$$\frac{\#bits}{\sec} = \frac{B}{N}\log_2\left(1 + \gamma \cdot \beta \cdot R^{-\alpha/2} \cdot N^{\alpha/2}\right) \tag{40}$$

and

$$\frac{\#bits}{\sec} = \frac{B}{N}\gamma \cdot \beta \cdot R^{-\alpha/2} \cdot N^{\alpha/2} \cdot \frac{1}{E_b/N_0}. \tag{41}$$

In the following section, the results of maximizing the expressions (40) and (41) are presented, including the values for optimal *NP* for subchannel networks.

5.3. Results

When maximizing expression (40), Shannon's limit of the data rate, over the number of channels *N*, the optimal number of channels *N* depends on the rank of the network *R* and the value of β. The results are presented in Table 3.

Table 3: Optimal number of subchannels for maximizing Shannon's data rate limit (40), as a function of improvement factor β and network rank R.

N		R											
		2	**3**	**5**	**10**	**20**	**50**	**80**	**100**	**150**	**200**	**300**	**500**
β[dB]	**0**	5	8	13	26	51	129	206	257	386	515	772	1286
	5	3	4	7	14	28	70	112	140	211	281	421	702
	8	2	3	5	10	20	49	78	98	146	195	293	488
	10	2	2	4	8	15	38	61	77	115	153	230	383

As seen in the table, the optimal number of subchannels is at least equal to 2, and it grows with the rank of the network. It also has a tendency to fall when the improvement factor β increases. One thing that cannot be seen from Table 3 is the spatial reuse factor. However, if the results from Table 3 are combined with formula (34), then it becomes clear that the *NP* of the subchannel network always tends to approach a fixed value that depends only on the improvement factor β, and not on the link length or the rank of the link (see Figure 23).

For example, for improvement multiplier $\beta = 0dB$, the network parameter tends to approach the value $NP = 0.35$, no matter how long the original link is, or how big the original rank of the link is. The value 0.35 of the *NP* of the subchannel network describes the spatial reuse in the subchannel network, and it means that if the link length is 35m, then the density of other transmitters around that link that operate in the same frequency is approximately one user in a square with 100m sides. In other words, one should not expect interferers in at least a square of side 100m around the link, which is an informal estimation. This gives a good sense of how densely populated the subchannel networks are, and what is the best spatial reuse strategy in the network of polynomial attenuation model with $\alpha = 3.8$.

The spatial reuse level is different for different values of improvement multiplier β. As users improve the values of β and effective *SINR*, it becomes more acceptable to have interferers closer to them, and more users can be packed in the same subchannel network. This reflects on the values of optimal *NP*. For $\beta = 5dB$ the optimal NP is

around 0.48, for $\beta = 8dB$ it is around 0.57, and for $\beta = 10dB$ it is around 0.64 (see Figure (23)).

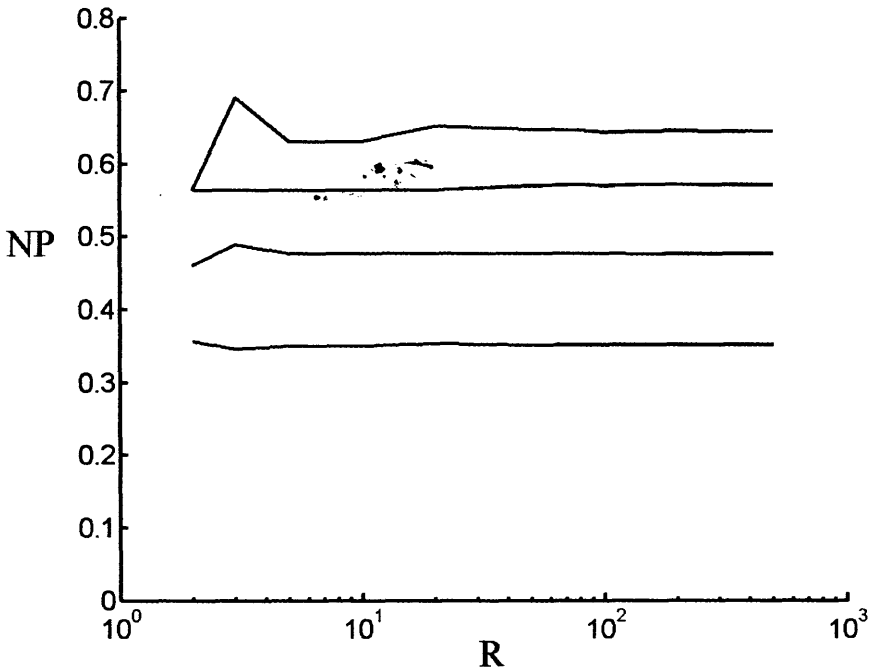

Figure 23: *Optimal values of* NP *in the subchannel network with maximum Shannon's data rate (40), vs. rank* R *of the original single channel network. The 4 plots correspond to, from bottom to top: β=0dB, β=5dB, β=8dB, and β=10dB.*

Shannon's data rate is not the only metric that can be used for estimating how many subchannels are needed in the network. The other approach described in this thesis estimates the data rate when the users use a fixed modulation scheme and choose which bit error rate to operate on, and is also a valid metric for the system performance. The data rate of such communication over a link is given by formula (41).

When one maximizes formula (41) with respect to N, the resulting optimal number of subchannels approaches infinity, and the corresponding data rate is also infinite. However, this result is limited by the practical implementation of the system. In particular, this result implies very few users in one subchannel, and the interference level in such subchannels then approaches zero value. That is the point where the assumption of negligible noise breaks down. Equation (41) stops being valid and the resulting data rate needs to be calculated by some other formula, including the thermal noise. The other limitation of this result is the fact that infinite number of subchannels means, all of the

subchannels are located in infinitesimally small bandwidths. In a practical implementation of the system, it would be very hard to make precise boundaries between different subchannels.

In conclusion, this chapter describes how the data rates of communication links in ad hoc wireless networks depend on the number of subchannels in the network. The number of subchannels that are needed in order to get the maximum data rate according to Shannon's limit is also determined by the value of *NP*. The network should always be divided into so many channels that the *NP* value corresponds to the values plotted in Figure 23. However, if the users in the network operate at some tolerable bit error rate, the optimal number of channels is infinite, or in other words, one per communication link. Even though this result breaks the model limitations and is not completely valid, it shows the tendency that more subchannels means greater data rate for all.

Chapter 6:

Summary, Conclusions, and Recommendations for Future Work

Ad hoc wireless networks are communication systems where the users do not have fixed positions, but instead are free to move in space, which is the advantage of such networks from the users' point of view, but at the same time creates problems in designing such networks. Some of the problems are on a high level, for example, multihop communication and routing protocols, but there are plenty of problems on a low level, such as single-hop protocols or the antenna design.

Standard configurations for ad hoc networks are yet to be determined and the research at RSEG is one of the attempts on achieving that goal. The two most important things in finding the best configuration are user satisfaction and the cost of implementation. Like in many other areas, there is a tradeoff between these two things. User satisfaction requires greater cost of implementation, and in order to find the best balance of these two things, one needs to know the tradeoff curve between them.

Research on these areas has been done but mainly in individual parts. For example, the problems of successive interference cancellation and protocols are being solved, but the whole picture of the network configuration still needs to be assembled. This thesis attempts to make some progress in that direction and integrates some of these individual parts.

The main goal of this thesis is to present a metric that captures the essence of user satisfaction, and that metric is chosen to be the data rate that the user is able to send or receive inside the network. Since this thesis is on the low level, singlehop communication is the focus, as opposed to multihop protocols and routing, which is the topic of other projects on ad hoc networks. This thesis also examines the effect of certain aspects of network configuration on the defined metric, which include successive interference cancellation, multiple antennas, and dividing the bandwidth into subchannels. These results present the positive effects of certain network components, and if the cost of

implementing those components is known, one can learn the tradeoff between user satisfaction and cost, which is the most difficult part of network design.

Ad hoc networks are hard to examine because of their free structure. Certain constraints had to be made, though, in order to estimate the data rate of individual users in the network. One of the constraints in this thesis was that users were uniformly and randomly distributed in the network with a fixed user-per-area density. This constraint implied that the interference level was a function of the density of users, and equal for all. Another important assumption was a polynomial path loss model $r^{-\alpha}$ with constant attenuation coefficient in all directions ($\alpha = 3.8$). However, that assumption is questionable since the path loss in real environments actually depends on the shape of the landscape and existence of objects between users.

As a consequence of these assumptions, a formula for user data rate was derived. That formula was then used to estimate the improvement of user satisfaction as one implements different system components. The three separate components that were examined in networks with single frequency channels were successive interference cancellation (SIC), multiple receiving antennas, and multiple transmitting antennas. These methods can be ranked in the following way. Multiple receiving antennas offered the best gain in the data rate. The two other, SIC and multiple transmitting antennas, had the same effect but less than multiple receiving antennas. In comparing SIC with the multiple antennas, the cases are equivalent for the same number of antennas as canceled interferers.

The part of the thesis on spatial reuse suggests the best number of frequency channels for the network. The resulting number of channels was dependant on the type of metric used. By Shannon's limit metric, the number of channels was the number that provided optimal network parameter (NP) level in the subnetwork of one channel. By the metric with fixed bit error rate and modulation scheme, the resulting number of channels was infinite, in other words, one per communication link, under the assumption of zero thermal noise.

These are the results of the thesis; however, further extensions are possible and needed for making the results more applicable to real systems. One of them is revising the path loss model in order to include the landscape characteristics. Some results, such

as [19] suggest heavy dependence of the attenuation coefficients on the street pattern in urban environments. That could be included in the existing polynomial attenuation model by distorting the network plane, so as to consider points along the street closer than they actually are, and points around the corners and across the block farther than they actually are. Assumption of uniform distribution of users in the network is also affected by this alteration and may need to be adjusted in that case.

Another possible extension could be to consider networks in 3 dimensions instead of 2 dimensions, as done in this thesis. If the signals had 3D paths then the antenna gain patterns in non-horizontal directions would also be important, and the multiantenna strategy and results would change. Other types of antennas, depending on the cost and performance characteristics, would then maybe replace isotropic dipole antennas. Isotropic dipole antennas are simple to make and maybe they would be still the best solution, but their best arrangement could be to orient them in various directions, instead of orientating them vertically, as done in this thesis. New experiments could then examine performance of such an antenna array.

The third extension could be to consider different techniques of using transmitting antennas for peaking up on the receiving end of the link. This thesis only examines what happens in the best case, when the transmitter knows how to adjust his array multipliers so as to achieve the highest signal power at the receiver. However, this is not easy to do in reality, especially in multipath environments, and since multiple transmitting antennas can only have near-perfect gain on the receiver, further research could examine the effects of different multiantenna usage strategies at the transmitting end of the link.

Protocols are another issue that could be incorporated into the work on user data rates. One of the protocol possibilities could be associated with space-time coding, since the communication link with multiple antennas at both the transmitter and the receiver makes up a MIMO system and space-time coding could improve its performance.

One more extension could be on the effects of non-perfect SIC, rather than perfect SIC. Even though realistic SIC techniques are not likely to have perfect cancellation, this thesis considered perfect cancellation. Further research could take into account realistic results of SIC and estimate the data rate improvement from them.

It would also be interesting to learn the cost of implementation of system components described in this thesis. That information would complement the results of this thesis on the benefits of those components, and together they would represent the tradeoffs in the network design.

Reference:

[1] P. Gupta, and P.R. Kumar, "The capacity of wireless networks," *IEEE Trans. Inform. Theory*, vol. 46, no. 2, March 2000.

[2] S. Verdu, "Optimum multiuser asymptotic efficiency," *IEEE Trans. Communications*, vol. Com-34, no. 9, September 1986.

[3] H.V. Poor, and S. Verdu, "Single-user detectors for multiuser channels," *IEEE Trans. Communications*, vol. 36, no. 1, January 1988.

[4] R. Lupas, and S. Verdu, "Linear multiuser detectors for synchronous code-division multiple-access channels," *IEEE Trans. Inform. Theory*, vol. 35, no. 1, January 1989.

[5] R. Lupas, and S. Verdu, „Near-far resistance of multiuser detectors in asynchronous channels", *IEEE Trans. Communications*, vol. 38, no. 4, April 1990.

[6] M. Honig, U. Madhow, and S. Verdu, "Blind adaptive multiuser detection," *IEEE Trans. Inform. Theory*, vol. 41, no. 4, July 1995.

[7] G.J. Foschini, D. Chizhik, M. Gans, C. Papadias, and R.A. Valenzuela, "Analysis and performance of some basic spacetime architectures," *IEEE J. Select. Areas. Commun., Special Issue on MIMO Systems*, pt. I, vol. 21, pp.303-320, April 2003.

[8] L. Greenstein, J. Anderson, H. Bertoni, S. Kozono, D. Michelson, and W. Tranter, „Channel and propagation models for wireless system design I and II," *IEEE J. Select. Areas. Commun.*, vol. 20, April/August 2002.

[9] A. Goldsmith, S.S. Jafar, N. Jindal, and S. Vishwanath, "Capacity limits of MIMO channels," *IEEE J. Select. Areas. Commun.*, vol. 21, no. 5, June 2003.

[10] D.W. Bliss, K.W. Forsythe, A.O. Hero, and A.F. Yegulalp, "Environmental issues for MIMO capacity," *IEEE Trans. Signal Processing*, vol. 50, no. 9, September 2002.

[11] D.W. Bliss, and A.M. Chan, "Outdoor PCS MIMO wireless communication channel phenomenology," *IEEE Trans. Antennas and Propagation*, August 2004.

[12] D.W. Bliss, "Robust MIMO wireless communication in the presence of interference using ad hoc antenna arrays," *Proceedings of MILCOM 03 (Boston)*, October 2003.

[13] S. Toumpis, and A. Goldsmith, "Ad hoc network capacity," *IEEE,* 2000.

[14] S. Toumpis, and A. Goldsmith, "Capacity regions for wireless ad hoc networks," *IEEE Trans. Wireless Communications*, vol. 2, no. 4, July 2003.

[15] S. Toumpis, and A. Goldsmith, "Performance, optimization, and cross-layer design of media access protocols for wireless ad hoc networks," *IEEE,* 2003.

[16] B. Hassibi, and B.M. Hochwald, "How much training is needed in multiple-antenna wireless links," *IEEE Trans. Inform. Theory*, vol. 49, no. 4, April 2003.

[17] W.C.Y. Lee, *Mobile Cellular Telecommunications*. McGraw-Hill 1995.

[18] D. P. Agrawal, and Q. Zeng, *Introduction to Wireless and Mobile Systems*. Thomson Brooks/Cole 2003

[19] X. Zhao, J. Kivinen, P. Vainikainen, and K. Skog, "Propagation characteristics for wideband outdoor mobile communications at 5.3 GHz," *IEEE J. Select. Areas. Commun.*, vol. 20, no. 3, April 2002.

[20] "Walfisch-Ikegami Propagation Model;"

http://www.awe-communications.com/Propagation/wal_ike/walike.htm.

[21] A.J. Rustako, Jr., V. Erceg, R.S. Roman, T.M. Willis, and J. Ling, "Measurements of microcellular propagation loss at 6 GHz and 2 GHz over non-line-of-sight paths in the city of Boston," *IEEE*, 1995.

[22] D.H. Staelin, Receivers, *Antennas, and Signals in Communication and Sensing Systems*.

[23] H. L. Van Trees, *Optimum Array Processing*, Part IV of *Detection, Estimation, and Modulation Theory*. Wiley-Interscience, 2002.